The stability of present-day Antarctic grounding lines — Part B: ~~Possible commitment~~ Onset of ~~regional collapse~~ irreversible retreat of Amundsen Sea glaciers under current climate on centennial timescales cannot be excluded

Ronja Reese[1,2], Julius Garbe[2,3], Emily A. Hill[1], Benoît Urruty[4], Kaitlin A. Naughten[5], Olivier Gagliardini[4], Gaël Durand[4], Fabien Gillet-Chaulet[4], G. Hilmar Gudmundsson[1], David Chandler[6], Petra M. Langebroek[6], and Ricarda Winkelmann[2,3]

[1]Department of Geography and Environmental Sciences, Northumbria University, Newcastle, UK
[2]Potsdam Institute for Climate Impact Research (PIK), Member of the Leibniz Association, Potsdam, Germany
[3]Institute of Physics and Astronomy, University of Potsdam, Potsdam, Germany
[4]Univ. Grenoble Alpes, CNRS, IRD, Grenoble INP, IGE, 38000 Grenoble, France
[5]British Antarctic Survey, Cambridge, UK
[6]NORCE Norwegian Research Centre, Bjerknes Centre for Climate Research, Bergen, Norway

Correspondence: Ronja Reese (ronja.reese@northumbria.ac.uk)

Abstract. Observations of ocean-driven grounding line retreat in the Amundsen Sea Embayment in Antarctica ~~give rise to~~ raise the question of ~~a~~ an imminent collapse of the West Antarctic Ice Sheet. Here we analyse the committed evolution of Antarctic grounding lines under the present-day climate~~conditions to locate the underlying steady states that they are attracted to and understand the reversibility of large-scale changes~~. To this aim, we first calibrate ~~the~~ a sub-shelf melt ~~module PICO~~ parameterisation, that is derived from an ocean box model, with observed and modelled melt sensitivities to ocean temperature changes, making it suitable for present-day simulations and future sea-level projections. Using the new calibration, we run an ensemble of historical simulations from 1850 to 2015 with ~~the Parallel Ice Sheet Model~~ a state-of-the-art ice sheet model to create model instances of possible present-day ice sheet configurations. Then, we extend ~~a subset of simulations best representing the present-day ice sheet~~ the simulations for another 10,000 years to investigate their evolution under constant present-day climate forcing and bathymetry. We test for reversibility of grounding line movement ~~if~~ in the case that large-scale retreat occurs. ~~While we find parameter combinations for which no retreat happens in~~ In the Amundsen Sea Embayment ~~sector, we also find admissible model parameters for which an irreversible retreat takes place. Hence, it cannot be ruled out that the grounding lines – which are not engaged in an irreversible retreat at the moment as shown in our companion paper (Part A, Urruty et al., in review) – will evolve towards such a retreat under current climate conditions.~~ we find irreversible retreat of Thwaites Glacier for all our parameter combinations, and irreversible retreat of Pine Island Glacier for some admissible parameter combinations. Importantly, an irreversible collapse in the Amundsen Sea Embayment sector ~~evolves on millennial timescales and~~ is initiated the earliest between 300 and 500 years in our simulations and is not inevitable yet ~~, but could become so if forcing on the climate system is not reduced in the future. In contrast, we find that~~ – as also shown in our companion paper (Part A, Urruty et al., in review). In other words, the region has not tipped yet. With the assumption of constant present-day climate the collapse evolves on millennial timescales, with a maximum rate of 0.9 mm/a sea-level equivalent ice volume loss. The contribution to sea-level by 2300 is limited to 8 cm with a maximum rate of 0.4 mm/a sea-level equivalent ice volume loss. Furthermore, when allowing ice shelves to regrow to their present geometry~~means~~, we find that large-scale grounding line retreat into marine basins upstream of the Filchner-Ronne ~~and Ross ice shelves~~ Ice Shelf and western Siple Coast is reversible. Other grounding lines remain close to their current positions in all configurations under present-day climate.

1 Introduction

The potential for the West Antarctic Ice Sheet (WAIS) to collapse in response to global warming was first raised as a concern ~~in~~ by Mercer (1978). This collapse would be driven by the Marine Ice Sheet Instability (MISI; Weertman, 1974; Schoof, 2007, 2012) and would raise global sea-levels by ~~more than~~ about 3 meters in the long term (Feldmann and Levermann, 2015a). Over the past decades, the Antarctic Ice Sheet has been losing mass (Smith et al., 2020) at an increasing rate (Shepherd et al., 2018; Rignot et al., 2019), with current mass losses being driven by buttressing loss of ice shelves through increased ocean-driven melting ~~(Paolo et al., 2015)~~(Gudmundsson et al., 2019). In particular, retreat of grounding lines – the boundary separating the grounded parts of the ice sheet from its floating ice shelves – and increased mass loss in the Amundsen Sea Embayment (ASE) sector (Rignot et al., 2019; Milillo et al., 2022) have raised the question of whether a collapse of the West Antarctic Ice Sheet driven by MISI might already be underway ~~(Rignot et al., 2014; Joughin et al., 2014; Favier et al., 2014)~~ (Rignot et al., 2014; Mouginot et al., 2014; Joughin et al., 2014; Favier et al., 2014). Several numerical modelling studies find continued retreat in the ASE under current climate conditions (Joughin et al., 2014; Favier et al., 2014; Seroussi et al., 2017; Arthern and Williams, 2017)~~and also the commitment of~~. Also, the commitment to large-scale retreat was found possible close to present-day climate conditions: Garbe et al. (2020) report that retreat of West Antarctic grounding lines could ~~be initiated by~~ occur at around $1-2$ °C of global warming above pre-industrial~~and~~, which would correspond to a regional warming of $1.8-3.6$ °C in the atmosphere and $0.7-1.4$ °C in the ocean surrounding the Antarctic Ice Sheet. Golledge et al. (2021) find that in a simulation ~~coming from~~ of the last interglacial, the West Antarctic Ice Sheet starts retreating after 1500 years with constant current climate conditions. These findings raise the importance of a systematic analysis to identify whether Antarctic grounding lines are *currently* engaged in an irreversible retreat due to MISI, and to gain a more detailed understanding of the committed retreat under present-day climate conditions, i.e., the steady state positions that current grounding lines are attracted to and the (ir)reversibility of potential large-scale transitions. Here and in an accompanying paper (Part A, Urruty et al., in review) we address these questions.

Urruty et al. (in review) show that ~~present-day Antarctic grounding line retreat is likely a ‘forced retreat’, meaning it is driven by external forcing alone rather than by the MISI instability mechanism~~ Antarctic grounding lines are likely not undergoing irreversible retreat due to MISI at the moment. ~~That no irreversible retreat is found in the current Antarctic geometry could be explained by two different underlying stability regimes of the system. Either MISI is in principle existent but not at play, or MISI is generally suppressed. The latter has been found to be the case in the presence of strong ice-shelf buttressing~~

~~(Gudmundsson et al., 2012; Pegler, 2018; Haseloff and Sergienko, 2018). The existence of tipping points due to MISI is thus a priori not clear for buttressed~~ Here, we investigate the stability regime of Antarctic grounding lines ~~located on retrograde bed slopes. The potential for irreversible grounding-line retreat in regions upstream of~~ under current climate forcing. We do this by simulating the evolution of the ice sheet under present-day ~~grounding lines has been shown in numerical simulations for the whole Antarctic Ice Sheet (Garbe et al., 2020), the West Antarctic Ice Sheet (Feldmann and Levermann, 2015a), the Wilkes subglacial basin in East Antarctica (Mengel and Levermann, 2014), and using high resolution modelling with an in-depth tipping analysis for Pine Island Glacier in the ASE sector (Rosier et al., 2021). The existence of tipping points for other grounding lines requires further investigation.~~

~~In this paper, we analyse the current trend in Antarctic grounding lines – observations show that they are clearly not in steady state at the moment – by investigating to which steady state positions grounding lines evolve towards under current climate conditions. If we find that the current climate commits grounding lines to large-scale retreat, we test if this retreat is reversible. To do so, constant present-day climate is applied in the simulations and no future changes in the climate conditions are included. This means that the simulations are~~ forcing, and then conducting a series of reversibility experiments, whereby we revert the forcing to pre-industrial conditions. The simulations are hence not projections, but rather allow us to assess the commitment of grounding line retreat under continued current climate forcing. ~~We discuss the possible ice sheet states and stability regimes in more detail in Section 4.3.1.~~ Note that we use ‘commitment’ here to refer to the evolution over timescales beyond the point of reference under constant climate conditions.

~~Firstly, we create a set of plausible model representations of the Antarctic Ice Sheet with the Parallel Ice Sheet Model (PISM). They are forced from 1850 to 2015 by historic changes in the ocean and atmosphere from a simulation of the Coupled Model Intercomparison Project Phase 5 to ensure that they replicate the present-day trend in mass loss. Sub-shelf~~ In our experiments, sub-shelf melt rates are calculated using the Potsdam Ice shelf Cavity mOdel (PICO; Reese et al., 2018a). Observed ongoing retreat in the ASE sector is linked to oceanic forcing (Jenkins et al., 2018) and recent projections underline the importance of the sensitivity of sub-shelf melting to ocean temperature variations (Jourdain et al., 2020; Seroussi et al., 2020; Reese et al., 2020). We thus calibrate the sub-shelf melt module PICO to represent observed (Jenkins et al., 2018) or modelled (Naughten et al., 2021) sensitivities of melt rates to ocean temperature changes. This is described in Section 2.

~~We then let the ice sheet states evolve under constant~~ Using the new PICO parameters, we create a set of plausible model representations of the present-day ~~climate conditions towards steady state and evaluate the corresponding committed grounding line movement. Note that a steady state reached this way is by construction stable. Also these experiments do not answer whether MISI is *currently* underway for Antarctic grounding lines but they instead explore whether an irreversible retreat might be committed to occur eventually under present-day climate conditions. To test for (ir)reversibility of grounding line retreat, we revert the climate conditions to pre-industrial and extend the simulations that show grounding line retreat by $20,000$ years. These experiments are presented in Section 3.~~

~~The results are then discussed in Section 4 and summarised in Section 5.~~

2 ~~Theoretical framing~~

~~We here discuss the potential states that Antarctic grounding lines could be in with respect to MISI. The terminology used for nonlinear systems is based on Strogatz (2018).~~ ~~**Schematic of potential stability regimes of Antarctic grounding lines.**~~ ~~Illustrated are possible present-day states of Antarctic grounding lines in (a) a schematic bifurcation diagram for the Marine Ice Sheet Instability and (b) a schematic diagram illustrating a fully reversible system, both represented by a system state and a control parameter. Black curve shows underlying steady system states (solid for stable, dashed for unstable). Tipping points or bifurcation points (red points) lie at the critical control parameter and critical system state. If MISI exists (panel a), the current, non-steady grounding line (indicated by crosses) might be at three qualitatively different locations relative to the steady-state curve and the tipping point. If no MISI exists (panel b), large-scale changes in the system state are reversible. In the companion paper, Part A (Urruty et al., in review), is is assessed whether the grounding line is currently undergoing MISI, by enforcing a steady state using a balanced-melt approach (grey curve). In this paper, Part B, we analyse the long-term evolution of the grounding lines (indicated by arrows) and their reversibility, i.e., whether large-scale retreat might be committed under constant climate forcing and if so, if this retreat is reversible.~~

~~MISI occurs when a positive feedback, where retreat of the grounding line increases the ice flow across the grounding line and this in turn causes further retreat, is at play. For a laterally uniform ice sheet, ice flow across the grounding line is a function of the local ice thickness which is linked through the flotation criterion to the bed topography. This means that due to the positive feedback, stable steady state grounding-line positions cannot exist on retrograde, in-land sloping beds (for constant bed properties and ice rheology; Schoof, 2007, 2012). In the presence of buttressing ice shelves, conditions are more complicated and it is possible that no MISI exists (Gudmundsson et al., 2012; Haseloff and Sergienko, 2018; Pegler, 2018). In the absence of buttressing, it was found that also a specific distribution of the basal friction parameter can allow for stable steady state grounding lines on retrograde sloping beds Brondex et al. (2017). Numerical modelling is then required to assess the state of the grounding lines.~~

~~MISI gives rise to hysteresis behaviour (Schoof, 2007) which can be visualised in a bifurcation diagram showing the system state, i.e., current location of the grounding line, with respect to the relevant control parameter, i.e., climate forcing in the atmosphere and ocean , see Fig. 7. Hysteresis means that over a range of control parameters, several possible steady states exist and thus the (evolution of the) current system state depends on its history. Those steady states can be stable or unstable, depending on whether a small-amplitude perturbation to the system is dampened (stable) or amplified (unstable) so that the system evolves back to its original steady state or away from it. At a bifurcation, or tipping point, a stable and an unstable branch merge, and if the system is moved beyond that point, it will engage in an irreversible transition towards the only existing stable state. Moving the system across a tipping point by changes in the control parameter is how tipping in marine ice sheets is generally thought to occur (this is called bifurcation-induced tipping, alternative ways that tipping can occur are discussed for example in Vanselow et al. (2022)). Such a transition is called 'irreversible', since reverting back to the original state requires the control parameter to be reduced substantially below the critical value until a second tipping point is crossed and the system irreversibly changes back to the first state. See Rosier et al. (2021) for a more detailed discussion.~~

~~Grounding lines in Antarctica show 'slow-onset' tipping (Ritchie et al., 2021) since also under very slowly increasing control parameters in quasi-steady experiments~~ Antarctic Ice Sheet with the Parallel Ice Sheet Model (PISM). The ice sheet states are forced from 1850 to 2015 with historic changes in the ocean and atmosphere from a simulation of the Coupled Model Intercomparison Project Phase 5 (CMIP5: Taylor et al., 2012) and their mass loss compared to observed trends. We then let the ice sheet ~~'s system state was found to evolve above the equilibrium curve, see Garbe et al. (2020) and Rosier et al. (2021). This means that crossing a critical threshold in their forcing (i.e., climate conditions) does not directly lead to an irreversible change in the their state (e. g., WAIS collapse). Instead, it is possible to have a temporary overshoot over the critical threshold without forcing the grounding lines to enter irreversible retreat (a relationship between time and amplitude for safe overshoots is derived for simple . Such states have been described as affording 'borrowed time' in which it is possible to revert to previous conditions before the undesirable system state locks in (Hughes et al., 2013). This is in line with Rosier et al. (2021) showing that critical slowing for MISI – which is a typical response for such a system approaching a tipping point (see also Scheffer et al., 2009) – only occurs when the critical system state is crossed, not the critical control parameter. It is also plausible since the mechanical, positive feedback related to MISI only kicks in once the critical system state (grounding line position)is crossed.~~

~~To summarise, present-day Antarctic grounding lines can either show no hysteresis behaviour (Fig. 7b), or, if hysteresis exists, they are in a transient state above or right of the upper stable branch of the underlying equilibrium curve (Fig. 7a, note that we focus on the upper stable branch here since we consider upstream tipping points). In the latter case, this means that an ice sheet, in particular under realistic forcing, does not necessarily cross the critical control parameter (i.e., climate conditions) and the critical system state (i.e., grounding line position) of a tipping point simultaneously.~~

~~Current grounding lines can hence be in principle in four qualitatively different positions in terms of MISI (see Fig. 7): **No instability:** MISI exists, and the grounding line has neither crossed the critical system state nor the critical control parameter. Letting the grounding line evolve with the control parameter kept constant, it would reach a stable steady state on the upper stable branch (following the dark blue arrow), and no tipping occurs. **Committed instability:** MISI exists, and the grounding line has crossed the critical control parameter, but not the critical system state. It is in an 'overshoot' state, i.e., it will evolve to the lower stable steady state branch but the collapse could still be prevented by reducing the control parameter below its critical value. However, if the control parameter is kept constant, it will eventually cross the critical system state and enter irreversible retreat~~ states evolve under constant present-day climate conditions. To test for (~~following the light blue arrow)~~ ir)reversibility of grounding line retreat, all simulations showing large-scale retreat are extended for another 20,000 years under (reverted) pre-industrial forcing. In a final step we analyse the transient evolution under current climate and reversibility of retreat over centennial timescales, to identify the onset of irreversible retreat. ~~Such a state is hence showing no instability at the moment, but an instability, or tipping, is committed under a constant control parameter. **Ongoing instability:** MISI exists, and the current grounding line has crossed the critical parameter and the critical system state. Such a state is undergoing irreversible retreat . Evolving this system forward under constant climate conditions the grounding line would, similar to the second case, retreatfurther until it reaches a new stable steady state (following the teal arrow). Such a state is considered to be tipped. **No MISI:** MISI is suppressed. The system might show large-scale changes for small changes in the control parameter, but these~~

~~are reversible.~~ These experiments are presented in Section 3. The results are then discussed and put into the wider context of tipping in Antarctica in Section 4 and summarised in Section 5.

~~The numerical stability analysis of our companion paper (Urruty et al., in review) analyses whether MISI is currently happening for any Antarctic grounding line. In that paper, a balance approach is used by which the surface mass balance is modified so that the current Antarctic grounding lines are in steady state (indicated by the grey curve in Fig. 7). Then, their stability is tested in a numerical stability analysis. If a stable steady state is found with respect to the modified surface mass balance, then the grounding line is likely not undergoing MISI in its current position or no MISI exists. But if an unstable steady state is found, then the grounding line is likely undergoing MISI in its current position. The study hence analyses the position of current Antarctic grounding lines with respect to the critical system state. Its findings can be interpreted to show that either case (1), (2) or (4) are likely true for all Antarctic grounding lines, and that case (3) can be excluded. Note that with this methodology, case (1), (2) or (4) cannot be distinguished.~~

~~The present paper can be understood to investigate the question whether the current Antarctic Ice Sheet is more likely to represent case (1), (2) or (4), i.e., whether present-day climate forcing commits the grounding lines to substantially retreat away from their current positions, or if they remain close to their current states. And if they retreat, if this retreat is reversible. In other words, this paper analyses the position of current Antarctic grounding lines with respect to the critical control parameter (i.e., climate conditions).~~

2 PICO parameter optimization

In this section, we introduce a new optimisation approach for the parameters in the PICO model in order to obtain suitable values for Antarctic model simulations~~, including projections of Antarctica's future sea level contribution. We~~ . The underlying idea is to select the model parameters such that the modelled sensitivity matches the sensitivity of melt rates to ocean temperature changes obtained from observations or numerical ocean modelling. In the following sections, we first describe the ~~methodology~~model, see Sect. 2.1, then how we obtain the melt sensitivity estimates for the Filchner-Ronne Ice Shelf (FRIS) and the Amundsen Sea ice shelves, see Sect. 2.2, ~~that~~ and finally how they are used as targets to select the PICO parameters in Sect. 2.3. ~~We then use this parameter set for all simulations conducted in this paper, using the ice sheet model PISM to investigate the commitment of grounding line retreat under present-day climate conditions.~~

2.1 PICO model

~~PICO calculates~~ We calculate sub-shelf melt rates ~~in ice-shelf cavities based on far-field ocean temperature and salinity~~using PICO. It extends the ocean box model (Olbers and Hellmer, 2010) for application in ice sheet models that resolve both horizontal dimensions. ~~We provide~~ The model input fields are far-field ocean temperatures and salinities~~to PICO which differ in~~ . They differ between 19 basins surrounding the Antarctic Ice Sheet and are derived from Schmidtko et al. (2014), similar to Reese et al. (2018a).

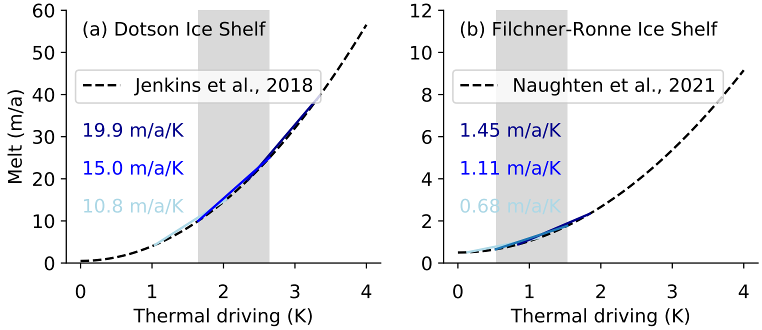

Figure 1. ~~**Target sensitivities for (a) Dotson Ice Shelf and (b) Filchner-Ronne Ice Shelf.**~~ **Sensitivities of melt rates to ocean temperature changes for (a) Dotson Ice Shelf and (b) Filchner-Ronne Ice Shelf.** Thermal driving is given as temperature relative to the surface freezing point and represents properties of the water masses at depth on the continental shelf in front of the ice shelf cavity. Melt is the average melt rate over the ice shelf in meter ice-equivalent per year. Dashed lines indicate estimations by Jenkins et al. (2018) and based on Naughten et al. (2021) as detailed in Appendix A1. ~~Grey~~ The grey bar indicates the range over which 'mean' linear sensitivity is ~~approximated~~calculated, using present-day thermal driving for the baseline temperatures. Coloured lines and numbers show the maximum, mean and minimum linear sensitivity estimates depending on the choice of present-day baseline temperatures (see Appendix A2).

~~PICO parameterises~~ In PICO the vertical overturning circulation in ice shelf cavities ~~and includes~~ is parameterised and a formulation of the ice-ocean boundary layer is included. For each of these processes, ~~PICO has one parameter~~one model parameter is required, which is constant across all Antarctic ice shelves. The parameter C influences the strength of the vertical overturning circulation, and the parameter $\gamma_T^\star$ describes the vertical heat exchange coefficient at the ice-ocean interface~~, which in reality depends on the ocean velocity and the ice roughness. In this paper we present a new optimization approach in which these parameters are selected such that the modelled sensitivity matches the sensitivity of melt rates to ocean temperature changes obtained from observations or numerical ocean modelling. In the following section we describe these targets and then present the parameter optimization in the section afterwards.~~ .

2.2 ~~Target melt~~ Melt sensitivity for Filchner-Ronne Ice Shelf and the Amundsen Sea Region

~~An analytical model of~~ Basal melt rates a_b, as calculated by PICO, are linear functions of input ocean temperatures T (Reese et al., 2018b, 2020). In the PICO model the slope of the ~~ice-ocean interface (Jenkins et al., 2018) and numerical models of idealised ice shelf cavities (Holland et al., 2008) suggests a quadratic dependency of ice shelf melting on ocean temperature changes. Temperature changes can equivalently be expressed in terms of thermal driving that is defined as the temperature above freezing point determined by local salinity and a reference pressure value, and both are used hereafter.For simplicity we use the surface freezing point, as the ice shelf draft (and therefore the in-situ freezing point) varies both in space and time.~~

~~We use the quadratic relationship~~ linear relationship, i.e. da_b/dT, depends on the value of the model parameters C and γ_T^*. While it has been argued that the dependency between melt rates and ~~ocean temperaturesobtained from~~ temperature may, more generally, follow a quadratic relationship (Holland et al., 2008; Jenkins et al., 2018) a sufficiently accurate linear approximation can be found for a given range of temperatures. By using observational data for Dotson Ice Shelf (Jenkins et al., 2018)~~as a target for the Amundsen Sea~~, see Fig. 1a~~. Doing so, we hope to represent the sensitivity correctly for small, warm cavities. For cold, large cavities, no observations spanning such a wide range of temperature inputs are available. Instead we use recent numerical ocean model simulations that include a switch from cold to warm conditions in~~ , and numerical model outputs for the Filchner-Ronne Ice Shelf cavity ~~(Naughten et al., 2021) and estimate a quadratic relationship from these~~from an ocean model (Naughten et al., 2021), see Fig. 1b, ~~with the procedure described in detail in Appendix A1.~~ we determine the values of the PICO model parameters to ensure that the sensitives of calculated melt rates to changes in ocean temperature are approximately the same over the range of expected temperature changes.

~~To get a sensitivity target for tuning PICO, we linearise the curves around present-day ocean temperatures. Note that PICO shows a linear sensitivity in particular for higher temperatures, because melting in PICO depends linearly on thermal driving and no dependency on the overturning velocity (which is also a function of thermal driving) is included in PICO. We first estimate the best, minimum and maximum present-day ocean input thermal driving in the respective region (see Appendix A2). Our best estimates~~ We use a temperature change of 1 Kelvin and our best estimates of the current baseline temperatures for FRIS and the ASE are 0.53 and $1.65^\circ\mathrm{C}$, respectively, and the minimum (FRIS: $0.13^\circ\mathrm{C}$, ASE:$1.04^\circ\mathrm{C}$) and maximum (FRIS: $0.84^\circ\mathrm{C}$, ASE: $2.34^\circ\mathrm{C}$) are taken ~~from~~ over all values in Table A1. ~~Those values are obtained by following the PICO procedure to average ocean conditions at depth over the continental shelf in front of the ice shelf cavity, which is a simplification that means that different water masses get mixed together and not only inflow water masses are considered (e.g. High Salinity Shelf Water which makes most of the inflow into the FRIS cavity would be at $0^\circ\mathrm{C}$ thermal driving with respect to the surface melting point). Since we are mainly interested in the melt rates provided to the ice shelf, we focus here on obtaining correct melt rates as well as melt sensitivities.~~

~~Then we derive the sensitivity between ice melt and baseline temperatures, using an increase in 1 Kelvin.~~ We test using a narrower or wider ~~interval for the linearisation and find~~ temperature change than 1 Kelvin and found that the baseline temperature ~~has~~ have a larger influence on the sensitivity~~than the temperature range over which it is linearised~~: for example, shifting the baseline temperature by 0.5 K gives a larger increase or decrease in the sensitivity than estimating the sensitivity over a temperature range of 0.5 or 2 K. We thus overall capture different ranges of the linearisation interval by using different input temperatures (best, min, max). ~~Sensitivities~~

By using both, estimates for the Amundsen Sea and Filchner-Ronne ice shelf, we represent the sensitivity of modelled melt rates to ocean temperature changes correctly for small, warm cavities as well as cold, large cavities. Note that no observations span a wide range of temperature inputs for Filchner-Ronne and this is why we use recent numerical ocean model simulation that includes a switch from cold to warm conditions in the cavity (Naughten et al., 2021), with the procedure to obtain the quadratic relationship described in Appendix A1.

Resulting sensitivities of melt rates to ocean temperature changes are added as text fields in Fig. 1.

For FRIS, we find a sensitivity of melt rates to ocean temperature changes between 0.7 and $1.5\ \mathrm{ma}^{-1}\mathrm{K}^{-1}$ with the best estimate being $1.1\ \mathrm{ma}^{-1}\mathrm{K}^{-1}$. Jenkins (1991) find an increase from 0.6 ma^{-1} to 2.6 ma^{-1} for a warming by 0.6 K using plume theory, which implies a higher sensitivity of 3.3 ~~for~~ $\mathrm{ma}^{-1}\mathrm{K}^{-1}$ for FRIS. Hellmer et al. (2012) report that a switch from cold to warm conditions increases average melt rates from 0.2 to 4 ma^{-1} for a warming of 2 K, which implies also a higher sensitivity of $1.9\ \mathrm{ma}^{-1}\mathrm{K}^{-1}$. From Comeau et al. (Fig. 9d and S10, 2022) we roughly estimate a melt sensitivity of $3.5\ \mathrm{ma}^{-1}\mathrm{K}^{-1}$. The order of magnitude is in all cases comparable. ~~We want to note here that currently no changes are observed in the ice streams in the Weddell Sea as have been reported for the ice streams in the ASE. Having the precisely correct sensitivity is hence less important for our study.~~

By comparison, the sensitivity of melt rates to ocean temperature changes for the ASE is higher (Fig. 1a). This might be due to the higher baseline temperatures and a larger slope of the ice shelf base (Jenkins et al., 2018). The sensitivity estimate based on the 'best' baseline temperature of $15\ \mathrm{ma}^{-1}\mathrm{K}^{-1}$ for Dotson Ice Shelf fits well with the estimate from Payne et al. (2007) for Pine Island Glacier Ice Shelf, which is $16\ \mathrm{ma}^{-1}\mathrm{K}^{-1}$. It is close to the initial sensitivity around $16\ \mathrm{ma}^{-1}\mathrm{K}^{-1}$ in Seroussi et al. (2017) for Thwaites Glacier Ice Shelf estimated from ocean simulations with ~~an~~ a $0.5\ \mathrm{K}$ temperature increase, see Fig. S5 in the Supplement of Reese et al. (2020). The sensitivity in the coupled simulation of Seroussi et al. (2017) decreases during the simulation~~with~~, reaching a minimum value of $4.5\ \mathrm{ma}^{-1}\mathrm{K}^{-1}$, and having a mean of $9\ \mathrm{ma}^{-1}\mathrm{K}^{-1}$ ~~, with the latter~~ that is more in line with the minimum sensitivity estimate.

~~Using these target sensitivities (min, best, max for FRIS and ASE), PICO parameters can be optimized as presented in the following section.~~

2.3 Results: PICO parameter selection

We select PICO parameters such that the ~~melt sensitivity~~ sensitivity of melt rates to ocean temperature changes is in line with estimates from the previous section and such that the underlying assumptions of PICO are met~~(similar to the approach in Reese et al., 2018a)~~. In total, we optimize five pairs of parameters that span the range of different target sensitivities in FRIS and the ASE presented in the previous section ~~. A summary of the results is given in Table 1.~~

~~We~~ ('min', 'max', 'best' in both regions and combining 'min' and 'max' of both regions). For the parameter optimisation, we conduct a parameter sweep ~~with PICO~~ for different values for C and $\gamma_T^\star$, see Fig. 2. ~~To have the melt rates calculated by PICO replicate present-day observations (in $\mathrm{Gt\,a}^{-1}$ from Adusumilli et al., 2020), we apply temperature corrections between -2 and 2 to the underlying present-day temperatures from Schmidtko et al. (2014) in each basin. This is similar to the approach used by Jourdain et al. (see Section 4.4 in 2020). Temperature changes of this order of magnitude almost span the entire variation of ocean temperatures observed in the Southern Ocean and large temperature corrections could point to missing assumptions in the melt calculation. However, we are here interested in the ice sheet response, and for the ice sheet it is overall important to have the correct melt rates in present-day as well as the correct increase in melt rates with ocean temperature changes, which is achieved by this method.~~

~~Note that PICO generally shows a linear melt sensitivity, but we still make sure to optimize temperature corrections and melt sensitivity consistently by first calculating the temperature correction for all parameter pairs $(C, \gamma_T^\star)$ tested, and then selecting the optimal parameter pair based on physical constraints on the corresponding melt rates and the resulting sensitivity estimates. With the parameter optimization, we thus obtain a set of two parameters $(C, \gamma_T^\star)$ and temperature corrections δT_b, for each basin $b \in 1, \ldots 19$ for each combination of target sensitivities.~~

Table 1. Results of PICO parameter optimization. We optimize parameters for five combinations of sensitivity targets (selected from 'best', 'min', 'max' for FRIS and ASE). For each pair of target sensitivities we summarise the baseline thermal driving TD used for the linearisation to obtain the target sensitivity $\frac{dm}{dTD}^{target}$ for FRIS and ASE. Parameters are evaluated based on the match of modeled sensitivities $\frac{dm}{dTD}^{PICO}$ with target sensitivities. Then we give the optimized PICO parameters C and $\gamma_T^{\star}$ which are similar for all Antarctic ice shelves. For details see Sect. 2.2 and 2.3.

sensitivity targets	TD (°C)	$\frac{dm}{dTD}^{target}$ ($\mathrm{ma^{-1}K^{-1}}$)	$\frac{dm}{dTD}^{PICO}$ ($\mathrm{ma^{-1}K^{-1}}$)	C ($\mathrm{Svm^3kg^{-1}}$)	$\gamma_T^{\star}$ ($\times 10^{-5}\mathrm{ms^{-1}}$)
FRIS best	0.53	1.11	~~1.20~~ 1.14	2.0	~~5.5~~ 5.0
ASE best	1.65	15.04	~~15.25~~ 14.61	2.0	~~5.5~~ 5.0
FRIS min	0.13	0.68	~~0.73~~ 0.72	1.0	4.0
ASE min	1.04	10.79	~~10.76~~ 11.11	1.0	4.0
FRIS max	0.84	1.45	~~1.59~~ 1.57	3.0	7.0
ASE max	2.34	19.91	~~19.49~~ 19.91	3.0	7.0
FRIS max	0.84	1.45	~~1.43~~ 1.42	3.0	4.0
ASE min	1.04	10.79	~~12.71~~ 12.99	3.0	4.0
FRIS min	0.13	0.68	~~0.89~~ 0.84	1.0	~~10.0~~ 9.0
ASE max	2.34	19.91	~~19.04~~ 18.56	1.0	~~10.0~~ 9.0

We select the best parameters using four criteria: (1) melting (no freezing) occurs in the first box of PICO close to the grounding line, (2) melting in the first box is larger than in the second, (3) the melt sensitivity for FRIS is close to the target from Sect. 2.2, (4) the melt sensitivity in the ASE is close to the target from Sect. 2.2. Criteria (1) and (2) are analogous to the original parameter selection of PICO in Reese et al. (2018a)~~. In the original selection, we also ensure that melt rates were comparable to observations in FRIS and the ASE. However, our aim here is to accurately capture the *sensitivity* of ice melt to temperature changes, as obtained by the new~~ , and we replace the criteria (3) and (4) ~~. To ensure that present-day melt rates are consistent with observations~~ of the original selection, which were to meet observed melt rates. To have the melt rates calculated by PICO replicate present-day observations (in Gt a^{-1} from Adusumilli et al., 2020), we apply ~~the temperature corrections . See Tables ?? to ?? for the corresponding~~ temperature corrections between -2 and ~~comparison with observed melt rates for each parameter pair.~~

2 K to the present-day temperatures from Schmidtko et al. (2014) in each PICO basin. This is similar to the approach used by Jourdain et al. (2020, see their Section 4.4). We optimize temperature corrections and melt sensitivity consistently by first calculating the temperature correction for all parameter pairs $(C, \gamma_T^{\star})$, and then selecting the optimal parameter pair. With the parameter optimization, we thus obtain a set of two parameters $(C, \gamma_T^{\star})$ and temperature corrections δT_b, for each basin $b \in 1, \ldots 19$ for each combination of target sensitivities. Table 1 shows that indeed for all combinations of ~~target~~ ASE and FRIS melt sensitivities, the sensitivities modelled by PICO with the respective, optimised parameters are generally in close agreement with the targets. See Tables S1 to S5 for the corresponding temperature corrections and comparison with observed

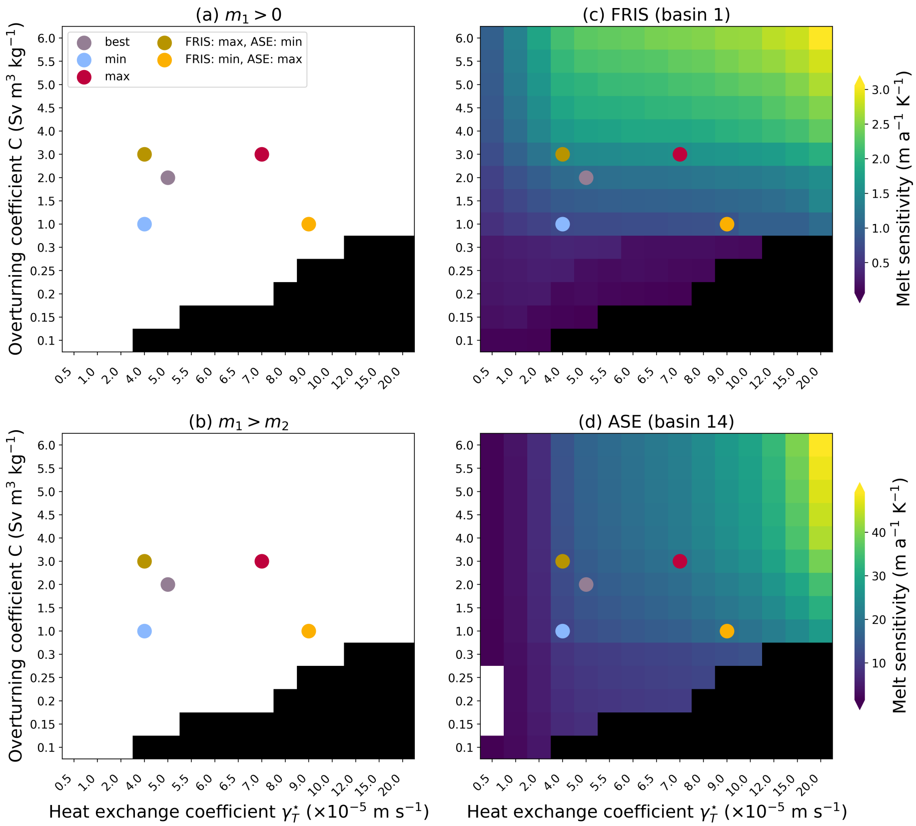

Figure 2. PICO parameter selection. Four targets are used for the optimisation of the heat exchange and overturning coefficients: (a) melting and not freezing in the first box close to the grounding line, which is true in the white areas~~,~~; (b) melt decreases away from the grounding line, i.e., melt rate in PICO box 1 is larger than in PICO box 2, which is true in the white colored areas; (c) sensitivity of FRIS melt rate to ocean temperature changes and (d) sensitivity of the ASE ~~, both match estimates from Sect. 2.2. The latter two criteria are depending on the baseline temperature for the~~ melt ~~curve~~rate to ocean temperature changes, which ~~can yield~~ both match best, min, max or mixed ~~sensitivities~~ estimates from Sect. 2.2 (indicated by dots). Note that parameter spacing on the x and y-axis is not equal and that the melt sensitivities to ocean temperatures modelled by PICO that are shown in (c) and (d) have ~~a~~ different ~~scale ranging over the modelled sensitivities in PICO~~scales. The ~~white~~ black boxes in (c) and (d) indicate regions where the criteria (a) and (b) fail.

melt rates for each parameter pair. In general, we ~~find that higher~~ can find temperature corrections that yield aggregated melt rates close to present-day estimates. Exceptions are basins 15 (Bellingshausen Sea) and sometimes 16 (George VI Ice Shelf), where temperature corrections of -2 K are not sufficient.

We find that the optimised PICO parameters range between 1 to 3 $\mathrm{Svm^3kg^{-1}}$ for C and 4 to 7 $\times 10^{-5}\mathrm{ms^{-1}}$ for $\gamma_T^\star$, with the best estimates being 2 $\mathrm{Svm^3kg^{-1}}$ and 5 $\times 10^{-5}\mathrm{ms^{-1}}$, respectively. In comparison with Reese et al. (2018a), we find overall higher parameter values: the value for C from the original tuning is now valid for a low sensitivity, while in all cases the value for the heat exchange is now higher. This is in line with a rather low sensitivity of melt rates to temperature changes found in the Antarctic projections of Reese et al. (2020). In general, we find that higher sensitivities require higher parameter values. ~~Sensitivities~~ The melt sensitivity to ocean temperature changes in the large-scale ice shelves such as FRIS ~~are~~ is dominated by the overturning coefficient, ~~which shows in~~ as indicated by the high value of C for high sensitivity targets in FRIS and low sensitivity targets in the Amundsen Sea. In the opposite case with a high sensitivity target in the Amundsen Sea and a low target in FRIS, we find that for the smaller ice shelves the heat exchange coefficient $\gamma_T^\star$ is more important. ~~In comparison with Reese et al. (2018a), we find overall higher parameter values: the value for C from the original tuning is now valid for a low sensitivity, while in all cases the value for the heat exchange is now higher . This is in line with a rather low sensitivity found in Reese et al. (2020).~~

Figure S2 shows the spatial pattern of melt rates for the 'min', 'mean' and 'max' PICO parameters. Generally, the modelled melt rates with PICO are higher close to the grounding lines and refreezing occurs in the large, cold cavities. Due to the box approach, melt rates are 'smoothed out' and show less spatial variability than observations Adusumilli et al. (2020). In the PISM experiments presented in the rest of the manuscript, the '~~best' fit parameters $C = 2$ and $\gamma_T^\star = 5.5 \times 10^{-5}$~~ min', 'best' and 'max' fit parameters are used.

3 Antarctic Ice Sheet simulations with PISM

In this section we describe the PISM simulations conducted using the newly optimised PICO parameters. We first describe the model and the experimental design ~~, see~~ (Sect. 3.1 and 3.2~~, then~~), and the ensemble of historic simulations ~~, see~~ (Sect. 3.3~~, and finally present results on~~). Then we present results of the long-term evolution of ~~Antarctica~~ Antarctic grounding lines under present-day climate conditions ~~, see~~ (Sect. 3.4), and analyse ~~their reversibility ,~~ the large-scale reversibility (Sect. 3.5). Finally, we look into the transient, centennial evolution and test reversibility over these time scales, see Sect. ~~3.5~~3.6.

3.1 PISM

The Parallel Ice Sheet Model (PISM; https://www.pism.io; Bueler and Brown, 2009; Winkelmann et al., 2011) is an open-source ice dynamics model ~~and is~~ developed at the University of Alaska, Fairbanks, and the Potsdam Institute for Climate Impact Research.

PISM is thermo-mechanically coupled and employs a hybrid of the Shallow Shelf Approximation (SSA) and Shallow Ice Approximation (SIA) to model ice flow. Temperatures within PISM are determined based on an energy-conserving enthalpy scheme including a thin subglacial water layer and a thermal layer in the bedrock (Aschwanden et al., 2012). A power-law relationship is applied between SSA basal sliding velocities and basal shear stress, with a Mohr–Coulomb criterion relating the yield stress to parameterized till material properties and the effective pressure of the overlaying ice on the saturated till (Bueler and van Pelt, 2015). Both, the grounding line and the calving front, are simulated at subgrid scale in PISM and evolve according to the physical boundary conditions. Basal friction is linearly interpolated on a sub-grid scale around the grounding line (Feldmann et al., 2014). ~~In order to~~ To improve the approximation of driving stress across the grounding line, the surface gradient is calculated using centered differences of the ice thickness across the grounding line. Sub-shelf melt rates are modelled using PICO and we use the set of optimal PICO parameters obtained with the new approach ~~for the 'best' baseline temperatures~~ (Sect. 2). In this study we conduct an equilibrium ~~spin up~~spin-up, and as a result glacial isostatic rebound is switched off, because it would require a paleo ~~spinup~~ spin-up to correctly reproduce representative present-day uplift rates. We do not apply sub-shelf melt in ~~partially floating grid cells~~ grounded grid cells that are partially floating and we only calve ice that extends beyond the present-day extent of the Antarctic ice sheet and ice shelves. Due to adaptive time-stepping and ~~the employment of the SIA and SSA~~usage of the superposition of the shallow ice and shallow shelf approximations, PISM is computationally efficient and capable of simulating large ensembles on multi-millennial time-scales.

3.2 Experimental design and initialisation

~~The primary aim of this manuscript is to analyse the long-term evolution of Antarctic grounding lines under current climate conditions. To do this, we first require initial configurations that represent the Antarctic Ice Sheet under present-day climate conditions. We then run these initial states forward in time, and let them evolve under constant atmospheric and ocean conditions.~~

The strategy adopted to build initial present-day ice sheet configurations with PISM relies on spin-up. We ~~test~~ account for uncertainties in model parameters by creating an ensemble of states and selecting a number of possible configurations that compare best to observations. For all ensemble members, we run historic simulations from 1850 to 2015 with the aim to reproduce current changes in ice sheet thickness.

To represent atmospheric and oceanic changes between 1850 to 2014 we use the historic forcing suggested by the Ice Sheet Model Intercomparison Project for CMIP6 (ISMIP6, Barthel et al., 2020; Seroussi et al., 2020), since no observations exist for that period in Antarctica. We apply the results from the Norwegian Earth System Model ~~(NorESM; Bentsen et al., 2013)~~ (NorESM1-M; Bentsen et al., 2013), one of the ISMIP6-suggested climate models. ~~The NorESM~~ While the NorESM1-M simulations do not provide a perfect representation of the past climate evolution, ~~but it was~~ they were found to have the smallest biases in the Southern Ocean and atmosphere (Barthel et al., 2020). Present-day ocean conditions are ~~given by the data of Schmidtko et al. (2014), which are~~ taken from Schmidtko et al. (2014), and then adjusted using the basin-wide temperature corrections from the PICO parameter optimisation presented in Sect. 2.3~~, and atmospheric~~. Atmospheric surface mass balance and surface temperatures are ~~used~~ from RACMOv2.3 (1995 to 2014 averages, van Wessem et al., 2018). Note that we apply the surface mass balance from the regional climate model directly and do not calculate melting in PISM internally with a positive-degree-day or equivalent model. These datasets are used for present-day climate, and anomalies are applied from the ~~NorESM-1~~ NorESM1-M output, following the ISMIP6 protocol. This approach captures transient changes in the atmosphere or ocean while linearly correcting biases. Ocean and atmosphere climate conditions for the ~~equilibrium~~ initial state in 1850 were obtained as follows: we first generate a timeseries of atmosphere and ocean anomalies from the modelled historic evolution that pass through zero anomalies between 1995 and 2014. We then add these anomalies to the present-day climatologies for the atmosphere and ocean which make sure that our forcing timeseries passes through the present-day dataset in the period between 1995 and 2014. Finally we take the average over the first 30 years of the respective timeseries to arrive at historic conditions. Note that the atmospheric forcing as provided by ISMIP6 starts in 1950 and we keep it constant at the 1950 to

1980 average between 1850 and 1950. In the following, we refer to the resulting atmospheric and ocean boundary conditions as ‘1850’ or ‘pre-industrial’.

Using these boundary conditions, the initial configurations are obtained as follows~~. Starting~~ : starting from BedMachine ice thickness and topography (Morlighem et al., 2020), PISM is run for 400,000 years with constant geometry and climate to obtain a thermodynamic equilibrium using a 16 km spatial grid resolution. ~~After this~~Then, an ensemble of simulations with varying model parameters is run for ~~several thousand~~ $25,000$ years towards dynamic equilibrium ~~on~~ at 8 km horizontal resolution using historic climate conditions ~~around~~ roughly representing 1850. We thus make the ~~conservative~~ assumption that the ice sheet was close to equilibrium in 1850, which was likely not the case. ~~Our assumption means~~ Note that any tipping point that might ~~be~~ have already been crossed due to climate changes prior to 1850 cannot be discovered with our methodology. However, starting from a state that is close to equilibrium in 1850 allows us to directly attribute any committed changes under present-day climate to the historic forcing.

The simulations employ 121 vertical layers with a quadratic spacing from 13 m at the ice shelf base to 100 m towards the surface. We vary parameters related to basal sliding~~and ice flow~~, in particular ~~we vary the SIA enhancement factor ($E_{SIA} \in \{1.5, 2\}$; Winkelmann et al., 2011), the~~ the till effective overburden fraction (~~$\delta \in \{1, 1.5, 2, 2.5, 3\}$~~$\delta \in \{1, 1.25, 1.5, 1.75, 2, 2.25\}$% Bueler and van Pelt, 2015), the decay rate of till water content ($C_d \in \{7, 10\}$ $\mathrm{mm\,a^{-1}}$; Bueler and van Pelt, 2015), and the ~~piecewise linear, parameterised till friction angle (smallest values $\Phi_{min} \in \{20, 24\}$are used for topography below -700m, largest values $\Phi_{max} \in \{30, 50\}$are used for topography above 500 or 1000m, respectively; Martin et al., 2011~~PICO parameters (‘min’, ‘best’ and ‘max’ from Sect. 2.3). This yields ~~40~~ 36 ensemble members to start with.

~~After 5000 years of model simulation, we select five ensemble members that compare best to present-day observations of ice geometry and speed (Morlighem et al., 2020; Mouginot et al., 2019) for the entire ice sheet,and for each of~~ From these, fifteen members were discarded as they showed a collapse of the ~~Amundsen, Ross and Weddell sea sectors. This makes 16 members in total due to overlaps between the best members for the different regions.~~West Antarctic Ice Sheet under pre-industrial conditions during the dynamic spin-up period. After the 25,000 year equilibrium spin-up we then use the remaining ensemble of 21 initial states to run historical simulations from 1850 to 2015 which are forced by changes in the ocean and atmosphere as described above. The corresponding changes in ocean temperature and salinity input for PICO are shown in Fig. S1. We assess the ensemble members in 2015 using a scoring method (Albrecht et al., 2020; Reese et al., 2020) that tests the root-mean-square deviation to present-day ice thickness (Morlighem et al., 2020), ice-stream velocities (Mouginot et al., 2019), as well as deviations in grounded and floating area ~~, and~~ (Morlighem et al., 2020), the average distance to the observed grounding line position ~~. We lay a specific focus~~ (Morlighem et al., 2020), and a comparison with present-day mass losses (Shepherd et al., 2018). We focus specifically on the Amundsen region, Filchner-Ronne and Ross ice shelves by additionally evaluating each indicator for these drainage basins individually. The ~~selected 16 ensemble members are then continued until they reach 25~~scoring of the present-day states is shown in Fig. B1 and all indicators are given in Table S6. We discard all ensemble members for which the modelled grounding line positions in 2015 in the Amundsen Sea deviate on average by more than 10 km from observations (see Table S6). This eliminates further six members leaving us with 15 remaining, ~~000 years. From these, seven members were~~

~~discarded due to ongoing advance in the large ice shelves or collapse of the West Antarctic Ice Sheet in the control simulations.~~

~~After the 25,000 year equilibrium spin up we then use the remainingensemble of nine initial states,~~ summarised in Table ~~??, to run historical simulations from 1850 to 2015 which are forced by changes in the ocean and atmosphere as described above. The corresponding changes in ocean temperature and salinity input for PICO are shown in Fig. S1. These runs are evaluated again, now including also a comparison with present-day mass losses in the metric. The scoring of the present-day states is shown in Fig. B1 and the best run is used for the experiments in Urruty et al. (in review)~~2.

While runs with PICO parameters that yield a higher sensitivity of melt rates to ocean temperature changes (i.e., 'max' and 'best' compared to 'min' parameters) have better scores, no such clear distinction can be found for the decay rate of till water. The lowest possible value of $\delta = 1.5\ \%$ yields worse scores than the other values. For this value, initial pre-industrial states that do not collapse exist only for the 'max' PICO parameters and the 'best' PICO parameters in combination with a higher till water decay rate (the latter was removed from the ensemble due to the large grounding line deviations in the Amundsen Sea). This parameter sets the fraction of the effective pressure of the overlaying ice on fully saturated till to the ice overburden pressure, see Bueler and van Pelt (2015). Lower values of this parameter yield more slippery bed conditions in particular for ice streams. Estimates from two ice streams indicate an upper limit of $0.7 \pm 0.7\%$ for the value of δ, mostly close to 1% (Engelhardt and Kamb, 1997; Blankenship et al., 1987; Smith et al., 2021), which supports the use of the lowest admissible parameter values of $\delta = 1.5\ \%$.

~~To understand the long-term evolution of Antarctic grounding lines, all these nine runs are then continued under present-day climate conditions for~~ We determine the steady state grounding line positions by continuing the runs for another 10,000 years (in total we run thus $25,000 + (2015 - 1850) + 10,000$ years). ~~To test the effect of uncertainties in present-day ocean temperatures, we add two simulations for one of the best-scoring initial states (second in Fig. B1, ANT2) with a stronger increase in ocean temperatures by +0.1 and +0.3 uniformly for all Antarctic ice shelves. To this aim we add the uniform temperature increase in the long-term evolution simulations after 2015. We~~ We also run control simulations with constant 1850 climate conditions parallel to all simulations to exclude that any remaining trends in the initial state ~~might~~ influence the results ~~,~~ (see Fig. B2~~.~~

~~To test for reversibility,~~). To test if the grounding line positions attained after 10,000 years are reversible to their current state, we revert the climate forcing back to the ~~1850-conditions in simulations in which we find large-scale retreat during these 10,000 years. We then extend those simulations for another~~ 1850 conditions. We ensure that the runs are carried on for sufficiently long time to arrive at a new steady state. We found that 20,000 years ~~with constant historic climate.~~ was a sufficiently long time period for this purpose. We also test reversibility by reverting back to pre-industrial forcing after 300, 500 and 1000 years of present-day forcing. We run those simulations over the same time as the present-day continued runs until year 12,015.

3.3 Results: Historic simulations and present-day ice sheet configurations

~~Modelled mass loss between 1850 and 2015, between 1992 and 2015, and drift in control run between 1850 and 2015 in mm SLE for the 9 ensemble members. This can be compared to observed mass loss of 7.6 ± 3.9 mm SLE between 1992 and~~

Table 2. PISM parameters ~~used for~~ of the ~~9~~ 15 ensemble members and modelled mass changes. Runs are sorted starting with the best scores shown in Fig. B1. ~~δ(%) ϕ_{min}(°) ϕ_{max}(°) h_{max}(m) E_{SIA} C_d(mm/a) ANT1 2.0 24.030.0500.02.0~~Given are modelled mass changes between 1992 and 2015, between 1850 and 2015 (both relative to the control run), and drift in the control run between 1850 and 2015 in mm SLE for all ensemble members. This can be compared to an observed mass loss of 7.6 ± 3.9 mm SLE between 1992 and 2017 (Shepherd et al., 2018). Furthermore, we summarise committed mass loss after 10~~ANT2 2.0 24.030.0500.02.07 ANT3 2.0 20.050.01000.02.010 ANT4 2.5 20.050.01000.02.010 ANT5 2.5 24.030.0500.02.010 ANT6 1.5 24.030.0500.02.07 ANT7 1.5 20.050.01000.01.57 ANT8 1.0 24.030.0500.02.07 ANT9 1.0 20.050.01000.02.07~~,000 years, relative to the control run, and the drift in the corresponding control run (in m SLE). Positive numbers indicate mass gain.

	δ (%)	C_d (mm/a)	PICO	$\Delta V_{2015-1850}$ (mm SLE)	$\Delta V_{2015-1992}$ (mm SLE)	$\Delta V_{CTRL,2015-1850}$ (mm SLE)	$\Delta V_{12,015-2015}$ (m SLE)	$\Delta V_{CTRL,12,015-2015}$ (m SLE)
AIS1	1.75	10	max	-7.35	-0.49	-7.03	-3.41	-0.22
AIS2	2.00	7	max	-10.06	-0.99	-5.02	-3.47	-0.17
AIS3	2.25	7	max	-5.44	-0.50	-4.28	-3.48	-0.19
AIS4	2.00	10	max	-6.39	-0.67	-5.45	-3.32	-0.23
AIS5	2.25	10	best	-1.88	1.39	-5.71	-3.17	-0.22
AIS6	2.25	10	max	-3.32	0.07	-7.00	-3.34	-0.23
AIS7	1.75	7	max	-7.54	-0.85	-5.96	-3.19	-0.20
AIS8	2.00	10	best	-3.56	0.67	-5.45	-3.10	-0.21
AIS9	2.25	7	best	-1.94	1.29	-5.30	-3.17	-0.21
AIS10	2.00	7	best	-1.61	1.32	-4.81	-2.93	-0.19
AIS11	1.50	10	max	-8.28	-1.54	-4.27	-3.25	-0.23
AIS12	2.25	10	min	-0.38	2.13	-5.47	-2.79	-0.22
AIS13	1.75	10	best	-3.35	0.66	-5.88	-3.00	-0.21
AIS14	2.00	10	min	-3.48	0.81	-4.58	-2.65	-0.26
AIS15	1.75	7	best	-8.17	-0.32	-5.54	-2.87	-0.19

~~2017. $\Delta V_{1850-2015}$ $\Delta V_{1992-2015}$ Drift $\Delta V_{CTRL,1850-2015}$ANT1-2.20 -2.59 5.07 ANT2-0.41 -3.50 3.31 ANT3-3.18 -2.66 4.93 ANT4-1.34 -2.83 4.36 ANT5-3.27 -2.99 4.52 ANT61.59 -1.31 3.99 ANT711.13 3.35 2.18 ANT816.33 3.53 7.93 ANT917.55 4.53 4.29~~ Starting from quasi-equilibrium states and 1850 climate conditions, we run all ~~nine~~ 15 members of the ensemble of initial configurations from 1850 to 2015 with changes in the ocean as well as the atmosphere as described in Sect. 3.2. ~~Figure 3~~ We refer to the initial states as 'quasi-equilibrium' states, since the initial simulations have not yet reached a full equilibrium, even after 25,000 years in their 1850 initial configurations, see Fig. B2 (maximum rate of -1.6 m/a ice thickness changes in single grid cells across all configurations, no spatial coherent patterns of ice thickness changes are found). We did control runs parallel to the historic simulations and for a further 10,000 years. During the historical simulations (years 1850 to 2015) the drift is 4-7 mm SLE, and during the 10,000 year extended simulations the drift is less than 26 cm SLE (see columns '$\Delta V_{CTRL,2015-1850}$' and '$\Delta V_{CTRL,12,015-2015}$' in Tab. 2). All runs remain close to their 1850 geometrical configuration.

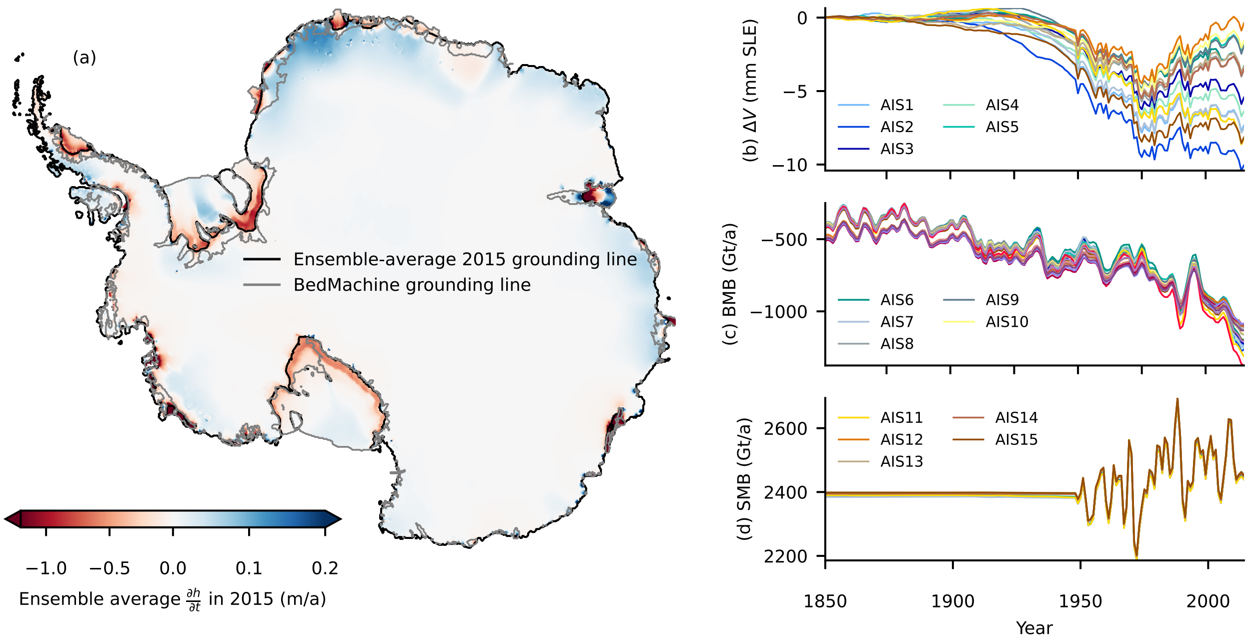

Figure 3. Historic simulations from 1850 to 2015 and present-day ice sheet configurations. Shown are (a) ensemble-average rates of ice thickness changes in 2015 (relative to control) with average grounding line position, and evolution of (b) the sea-level relevant ice volume (in millimetres sea-level equivalent, mm SLE), (c) basal mass balance of ice shelves (excluding melting in grounded regions), and (d) surface mass balance (both in gigatons per year).

Figure B2 shows that grounding lines move only a little for the ensemble and that rates of volume change monotonically decrease towards zero. In the following, results are presented relative to the respective control runs unless stated otherwise.

Figure 3a presents the results at the end of these historical simulations (2015) and shows that in 2015, the rates of ice thickness change averaged over all ensemble members generally resembles the observed pattern, see for example ~~Smith et al. (2020)~~ ~~.~~ Fig. 3 in Smith et al. (2020). This is also true for individual ensemble members. In general, thinning occurs in accordance with observations in the Amundsen and Bellingshausen Sea sectors, along the Antarctic Peninsula and for Totten and Moscow-University ice shelves. Also in line with observations, thickening due to increased snowfall is found in the interior of the ice sheet. ~~In~~ However, in contrast to observations, the simulations also show thinning in and upstream of Ross, Filchner-Ronne and Amery ice shelves and in some places along Dronning Maud Land because of ocean temperature increases in these areas. This ~~might not be representative of actual ongoing changes since coarse-resolution climate models cannot fully resolve the important processes on the continental shelf. This~~ discrepancy from observations must be taken into account when interpreting the results of the long-term simulations.

Grounding line positions and ice thickness differences to present-day observations are shown in Fig. S3, the ensemble-average grounding line position in Fig. 3a. All runs show grounding lines for Filchner-Ronne and Amery ice shelves that are extended seaward of observations. Furthermore, runs show a retreated grounding line in the Siple Coast of Ross Ice Shelf which is a problem encountered often in spin-up as this region is close to flotation. Overall, this suggests that our results for the long-term evolution in the next section overestimate changes in the cold cavity ice shelves like Ross and FRIS.

While the pattern of thinning and thickening is overall comparable with observations, the thinning rates in the ASE sector are ~~rather low~~ lower and do not extend as far inland ~~as in observations~~Smith et al. (2020). As a result, simulated integrated mass losses for present-day (see column ‘ $\Delta V_{2015-1992}$’ of Table 2 and Fig. 3b) are generally at the lower end of observations of ~~7.6 ± 3.9~~ 7.6 ± 3.9 mm SLE between 1992 and 2017 (Shepherd et al., 2018). ~~Six of nine ensemble members shows~~ Eight out of fifteen ensemble members show no mass loss or even mass gain in that period~~, see also Table 2. There are several possible reasons for this: snowfall increases might be too high, the effect of calving and damage is missing in the simulations, changes in the ocean forcing or translation to basal melting might be too weak, we apply no melt in partially floating grid cells at the grounding line. Higher mass loss might be expected with higher resolution < 8 km, also particularly mass loss~~. Particularly, mass loss at Pine Island Glacier (PIG) is lower than in observations~~, potentially due to the rather coarse resolution or its grounding lines being downstream of the observed position~~. Overall, this suggests that our results for the long-term evolution in the next section ~~overestimate changes in the cold cavity ice shelves like Ross and FRIS and~~ underestimate changes in the ASE.

We find that ~~the magnitude of mass loss depends strongly on sliding parameters . This~~mass loss is higher for PICO parameters that yield a higher sensitivity of melt rates to ocean temperature changes (‘max’), and for lower values of the sliding parameters ($\delta = 1.5, 1.75\%$) and till water decay rate ($C_d = 7$) that both yield more slippery bed conditions. Such a dependency on sliding parameters, as well as a dependency on the choice of the sliding law, has been found also in previous studies ~~(Brondex et al., 2019)~~(Brondex et al., 2019; Albrecht et al., 2020). Higher mass ~~losses occur for lower values of δ which is a parameter defining the fraction of the effective pressure on the till to the ice overburden pressure for fully saturated till. Lower values of this parameter yield more slippery bed conditions in particular for ice streams, in line with a stronger response to buttressing loss through increases ocean-driven~~ loss for the ‘max’ PICO parameters in comparison to the ‘best’ and ‘min’ parameters are expected as those parameters yield higher changes in sub-shelf ~~melting. However, those simulations tend to have the grounding line of Thwaites Glacier upstream of present-day (see Fig. S3).~~ melt rates for the same historic ocean changes applied in all simulations.

~~All runs show grounding lines for Filchner-Ronne and Amery ice shelves that are extended seaward of observations. This is maybe an artefact of creating an equilibrium state at 1850 climate conditions, a problem with the initial climate used or with the coarse sampling of water masses in PICO. Furthermore, runs show a retreated grounding line in the Siple Coast of Ross which is a problem encountered often in spin-up as this region is close to flotation.~~

Generally, sub-shelf melt increases from 1850 onward to values between ~~900 to 1200~~ 1000 to 1400 $\mathrm{Gta^{-1}}$ in 2015, ~~comparable to~~ see Fig. 3c, slightly lower than observations ranging between 1173.1±148.5 $\mathrm{Gta^{-1}}$ in 1994, 1,570±140 $\mathrm{Gta^{-1}}$ in 2009 and 1,160±150 $\mathrm{Gta^{-1}}$ in 2018 (Adusumilli et al., 2020). Differences between ensemble members occur due to different ice shelf extents in the initial states. Our historic simulations do not replicate the particularly high melt fluxes in 2009 which may be a reason why overall mass losses are at the lower end of observations.

Surface mass balance varies only from 1950 onward since no data were available beforehand~~and extended constantly back in time.It is more~~ , and is held constant during 1850 to 1950, see Fig. 3d. It is similar for all ensemble members since the maximum ice extent is pre-defined based on BedMachine Antarctica and the integrated surface mass balance is hence similar for all members.

~~We note that the control simulations do yet not reach a full equilibrium, even after 25,000 years in their 1850 initial configurations, see Fig. B2. We continue the control runs parallel to the historic simulations and for further 10,000 years. During the historical simulations (years 1850 to 2015) the drift is 2-8 mm SLE (see Tab. 2). Only runs that remain close to their 1850 configuration are used here. Figure B2 shows that grounding lines move only a little for the ensemble presented and that rates of volume change monotonically decrease towards zero.~~

3.4 Results: Long-term, steady-state grounding line ~~evolution~~ positions under present-day climate conditions

~~Committed mass loss after 10,000 years (in m SLE).~~ ~~$\Delta V_{12,015-2015}$(m SLE) ANT1-0.76 ANT2-0.81 ANT3-0.77 ANT4-0.69 ANT5-0.59 ANT6-0.89 ANT7-2.84 ANT8-2.48 ANT9-2.23 ANT2 ΔTD = 0.1 K-1.49 ANT2 ΔTD = 0.3 K-4.15~~ We investigate the long-term evolution of present-day Antarctic grounding lines by keeping the present-day climatology constant following the historic simulation and letting the ice sheet state evolve towards a new equilibrium for 10,000 years. Note that 10,000 years might not be sufficient to reach a full equilibrium, but we get a clear indication of what such an equilibrium state might look like. We then investigate if the grounding lines remain close to their currently observed position or if they retreat substantially.

Figure 4 shows that the grounding lines of the present-day configurations retreat ~~in some simulations~~ substantially in the marine regions of West Antarctica over the 10,000 years with constant climate conditions. Overall, mass loss ranges between ~~60 and more than 4 m SLE , which is lost over~~ 2.7 m and 3.5 m SLE (see column '$\Delta V_{12,015-2015}$' of Table 2) with the maximum rates of ice loss over the 10,000 ~~years (see Table ??) . Note that most~~ years ranging between 0.7 $\mathrm{mm/a}$ for AIS14 to 0.9 $\mathrm{mm/a}$ sea-level equivalent ice loss for AIS11. For comparison, the drift in the historic initial states over this period is less than 30 cm. Note that some states are still losing ice at the end of the simulation time, and thus grounding lines might not have converged fully to a new stable steady state position~~.~~, see Fig. S4. This is most prominent for AIS1-AIS6 and AIS12 which mostly show continued mass loss in Pine Island (except for AIS6 which shows no retreat of Pine Island Glacier but further retreat in the region connecting Thwaites and Ross).

~~Substantial~~ Grounding line retreat and the associated loss of large parts of the marine basins is found in the ASE sector, upstream of Thwaites Glacier ~~. This occurs for ensemble members with more slippery bed conditions or higher ocean temperatures. Grounding lines and ice thickness changes~~ and in some cases upstream of Pine Island Glacier. Grounding lines for the individual ensemble members are shown in Fig. S4. ~~Ensemble members that show this widespread collapse are ANT7, ANT8 and ANT9, which have lower δ parameter values. Also, the run testing a +0.3 higher ocean forcing for a non-collapsing state ANT2 with more rigid bed conditions shows collapse. Note that the more slippery ensemble members have present-day grounding lines upstream of their present-day locations for Thwaites Glacierand, at the same time, are better at reproducing present-day observed mass losses.~~

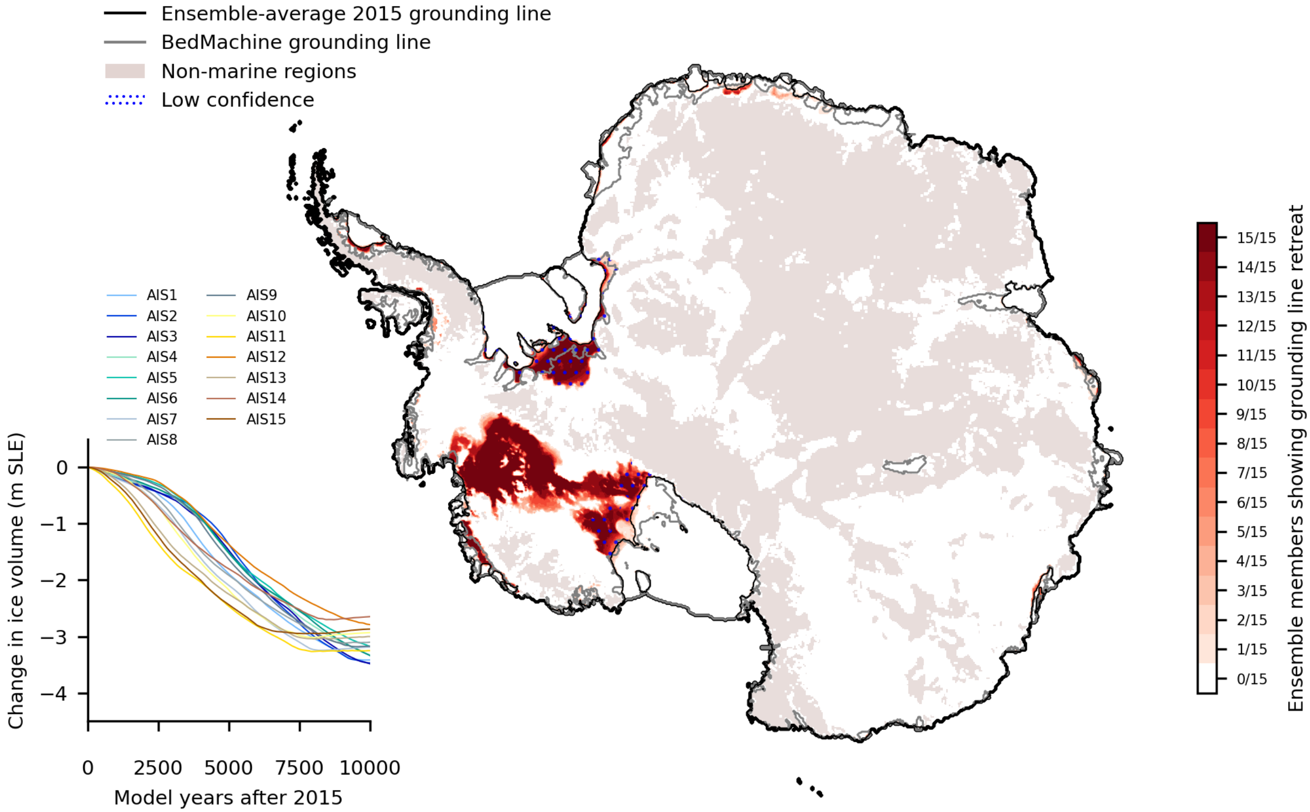

Figure 4. Long-term evolution of present-day Antarctic grounding lines under constant present-day climate conditions. Starting in ~~present-day~~ present day after the historic forcing from 1850 to 2015, simulations are continued with constant present-day climate for 10,000 years. Red colors show regions over which the grounding line retreats. The darker the red, the more ~~simulations~~ model configurations show grounding line retreat over the respective region ~~in the different simulations corresponding to variations in basal sliding and ice flow parameters~~ (retreat is plotted in comparison to a control simulation). Black contour shows ensemble-average initial grounding line position in 2015. Inset shows the evolution of sea-level relevant ice volume for all ensemble members (m SLE, metres sea-level equivalent, relative to the drift in the initial state over that period). Dots on retreat areas indicate regions in which present-day modelled thinning ~~deviates from~~ is inconsistent with observations (namely for ~~FRIS~~ Filchner-Ronne and Ross ice shelves). Light brown indicates bedrock above present-day sea level, white areas indicate bedrock below sea level. ~~Note that retreat occurs only in marine regions which have bedrock below sea level.~~

~~The experiments with increased ocean forcing were conducted using one of the initial states that best replicated observations. The state itself shows limited retreat of the the grounding lines over the 10, 000 years. However, smaller tipping points might be crossed, as discussed in the case of Dotson and Crosson ice shelves in the companion paper (Urruty et al., in review). We~~

~~find that for +0.1 K higher ocean temperatures in present-day substantial retreat occurs in FRIS and Ross Ice Shelf, but not in the Amundsen Sea. For +0.3 K higher present-day ocean temperatures, WAIS collapses from both directions, the Amundsen and the Ross Seas. This indicates that large-scale retreat of all marine regions in West Antarctica is very sensitive to small changes in the ocean temperatures.~~

All states except for AIS6, AIS10 and AIS15 show partial (AIS7) or substantial retreat of Pine Island Glacier. For a large number of these states this connects to the retreat in Thwaites (AIS1, AIS2, AIS3, AIS4, AIS5, AIS9, AIS11, AIS12). ~~No retreat of Pine Island Glacier upstream of its present-day position is found. However, as~~ As discussed in the previous section, Pine Island Glacier's grounding line is too far downstream (around 50km) of present-day in all ensemble members, and modelled present-day thinning rates are too low in comparison with current observations. We ~~think that a more detailed high-resolution modelling study would be required to analyse the committed evolution of Pine Island Glacier. We~~ find some retreat in Smith, Kohler and Pope glaciers, which does, however, not extend very far upstream of the present-day grounding line positions.

We find that all ensemble members retreat in the ~~regions that span between the~~ Robin subglacial basin and towards the ice rumples ~~in~~ of the Ronne Ice Shelf that ~~was~~ were grounded in the initial states although it is floating in observations. ~~However, only about half of the runs continue~~ All runs show retreat that continues beyond present-day grounding line positions. As we discussed in the previous section, this region shows thinning after the historic simulation which is not in line with observations. ~~This hints at an issue with the historic ocean forcing in this area, which could be the general circulation model simulation, but also that PICO does not modify water masses on their way into the cavity and translates all changes on the continental shelf in front of the cavity directly into changes in the cavity.~~

Grounding lines retreat for almost all members of the ensemble in the Siple Coast of Ross Ice Shelf ~~. Simulations with more slippery bed conditions show stronger retreat.~~ in the 10,000 years. Similar to FRIS, the historic runs show thinning in this region which is not compatible with observations. All runs except AIS6 show a connection between Thwaites Glacier and Ross Ice Shelf. A retreat of Thwaites can also indirectly trigger retreat in Ross as discussed for an idealised system in Feldmann and Levermann (2015b). Further work is required for both ice shelves with large, cold cavities to understand current climate forcing and committed retreat.

In all other regions of Antarctica we find only small retreat of grounding lines ~~.~~ (less than 25 km in the 10,000 years).

3.5 Results: ~~Reversibility~~ (Ir)reversibility of large-scale retreat

~~To test for the reversibility of large-scale retreat found in four ensemble members in the previous section~~To test whether large scale retreat after 10,~~we reverse~~ 000 years (see previous section) is (ir)reversible, we revert climate forcing back to pre-industrial ~~, 1850~~ conditions and extend the ~~four simulations that show large-scale retreat~~ simulations for another 20,000 years. Reversibility experiments that we did at earlier points in time to narrow down the onset of irreversible retreat are discussed in the next Sect. 3.6. Figure 5 (a) summarises reversibility for all runs; individual results are shown in Fig. S5 which also shows that rates of ice thickness change ~~in~~ at the end of the reversibility runs are small enough to consider the grounding lines close to steady state. We find that retreat in Thwaites Glacier shows overall no reversibility with the reversed grounding line ~~usually~~ close to the collapsed one in all ~~four simulations. In the ANT7 and ANT2+0.3 simulations~~ simulations. Pine Island Glacier

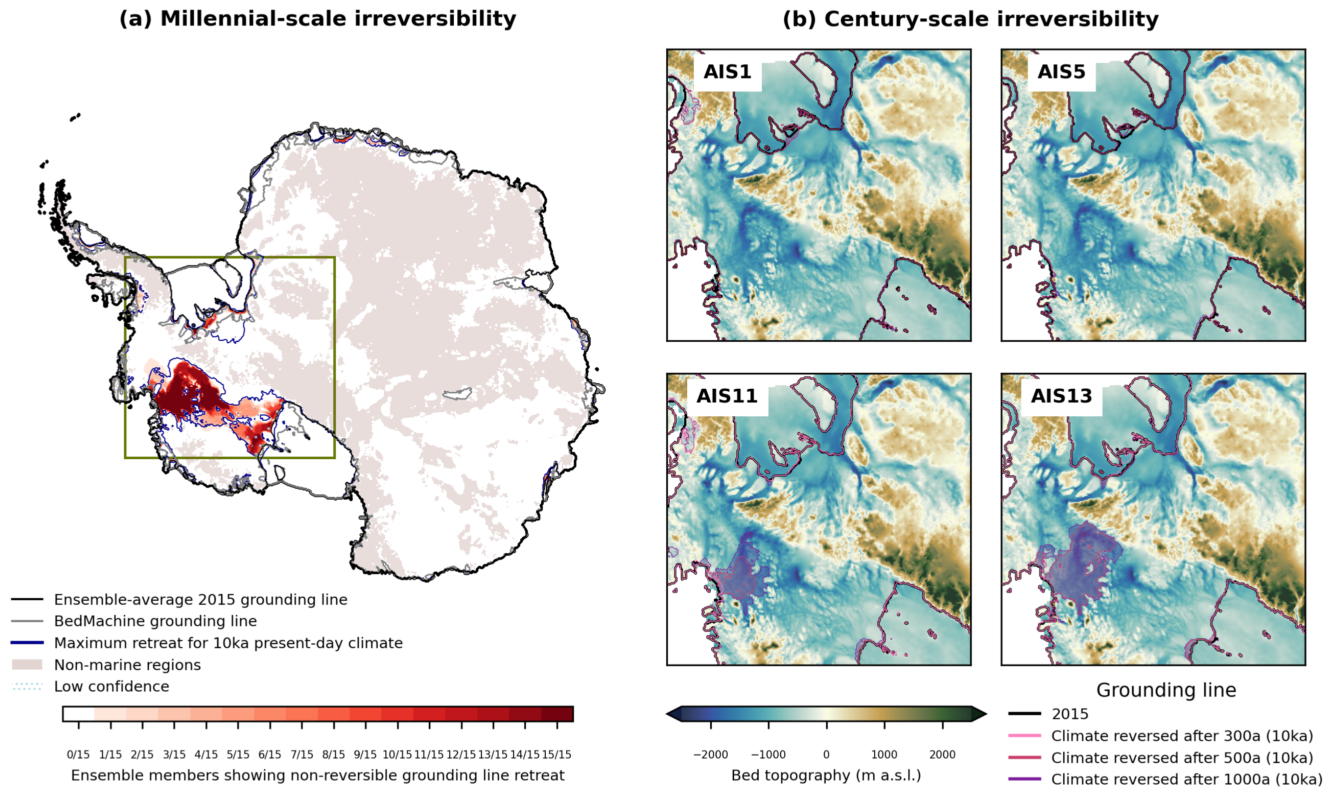

Figure 5. ~~**Reversibility experiments of large-scale retreat in West Antarctica.**~~ ~~Four present-day configurations~~**Reversibility experiments of large-scale retreat.** (a) Millennial-scale experiments. Red areas show regions that remain ungrounded after 20,~~with their 2015 grounding lines shown in black~~000 years of (reverted) historical climate following the 10,~~show large-scale retreat under~~ 000 years of constant present-day climate ~~(red~~ that caused grounding lines ~~show~~ to retreat (see Fig. 4). The maximum extent of grounding line ~~positions~~ retreat after 10,000 years ~~)~~constant climate is shown in blue. The darker the red, ~~see also~~ the more potential present-day configurations show irreversible grounding line retreat over the respective region. Other labels as in Fig. 4. Box shows the zoom of the right panels. (b) Centennial-scale experiments. Four present-day configurations of Antarctica, with their 2015 grounding lines shown in black, are integrated forward under constant present-day climate. When reversing the climate to historic conditions ~~for 20~~after 300, ~~000 years~~500, and 1000 years in the simulations, grounding lines evolve to the ~~positions~~ locations shown in ~~blue~~the map (positions in year 12015); differences to present-day grounding lines are indicated by shading. The ~~spatial~~ base map shows the ~~rate of ice thickness change after~~ bed topography from BedMachine (Morlighem et al., 2020). We here show the ~~20~~best ensemble member (AIS1), ~~000 years~~ the best ensemble member for 'mean' PICO parameters (AIS5), and two examples, AIS11 and AIS13, that show centennial onset of ~~reversal~~irreversible retreat.

shows reversibility of the grounding line to their 2015 positions in some simulations (AIS8, AIS9, AIS12), the grounding line ~~shows some advance~~advancing to intermediate locations in some (AIS1, ~~but halts substantially upstream from its current position~~ AIS2, AIS3, AIS4), as well as no advance (AIS5, AIS11, AIS13) or continued retreat (AIS14) in others. This could indicate that several regions of irreversible retreat (and tipping points) exist, in line with Rosier et al. (2021), and that in some cases the reduction in the forcing is sufficient to ‘jump’ back across all tipping points to the initial grounding line position while in others, not all or none of the tipping points can be reversed. In contrast, FRIS shows ~~a~~ clear reversibility, ~~with~~ where the grounding line ~~advance~~ re-advances to almost its present-day or historic position in the initial configurations ~~. The~~ in all cases. The western Siple Coast in Ross Ice Shelf ~~shows also reversibility in all four cases~~ also shows reversibility, with the grounding line reaching a position slightly upstream of the modelled present-day location ~~.~~ once the connection to Thwaites has become grounded. Where the ice shelves remain connected, the grounding lines in Ross do not reverse, or re-advance to intermediate positions. The eastern Siple Coast shows irreversible retreat in most cases and remains retreated.

3.6 Results: Transient evolution on centennial time-scales

We furthermore test the reversibility at earlier stages of the simulation and analyse the ice sheet evolution over the initial 300 years. This is shown for four examples with different behaviour in Fig. 5 (b), all reversibility runs are shown in Fig. S4. We test reversing the climate conditions to pre-industrial conditions after 300, 500, and 1000 years of constant present-day condition and extend the runs until year 12,015. Doing so allows us to narrow down the onset of irreversible retreat. Until year 300, none of our simulations show irreversible retreat, since when reversing the forcing back to pre-industrial conditions, the grounding lines stay in their location or re-advance to their pre-industrial positions. However, when reversing after 500 years, AIS11 shows continued retreat of Thwaites glacier and AIS13 shows continued retreat of Thwaites and Pine Island Glaciers. The same is true for another initial configuration (AIS15). When reversing after 1000 years, additionally AIS14 shows continued retreat. The continued retreat indicates the onset of irreversible retreat prior to the respective time. This is also visible from the evolution of the ice volume, see first column of Fig. 6. To summarise, we find that 3/15 ensemble members show an onset of irreversible retreat between 300 and 500 years of constant present-day climate conditions and 11/15 show no onset of irreversible retreat within 1000 years. This shows that the timescale at which irreversible retreat starts is dependent on the model parameters of the initial configuration.

In addition, we analyse the rates of ice loss and the total ice loss. In the first 300 years of the simulations with constant present-day climate starting in 2015, we find an increasing rate of volume loss with a maximum rate of 0.4 $\mathrm{mm/a}$ leading to 8 cm of sea-level equivalent mass loss, see Fig. 6.

4 Discussion

In the following sections, we discuss the optimization of PICO parameters, see Sect. 4.1, and the PISM experiments~~.~~, see Sect. 4.2. Based on these, we then ~~draw conclusions on the potential states of Antarctic grounding lines discussed in~~ discuss tipping in Antarctica with respect to MISI in Sect. ~~4.3.1~~4.3.

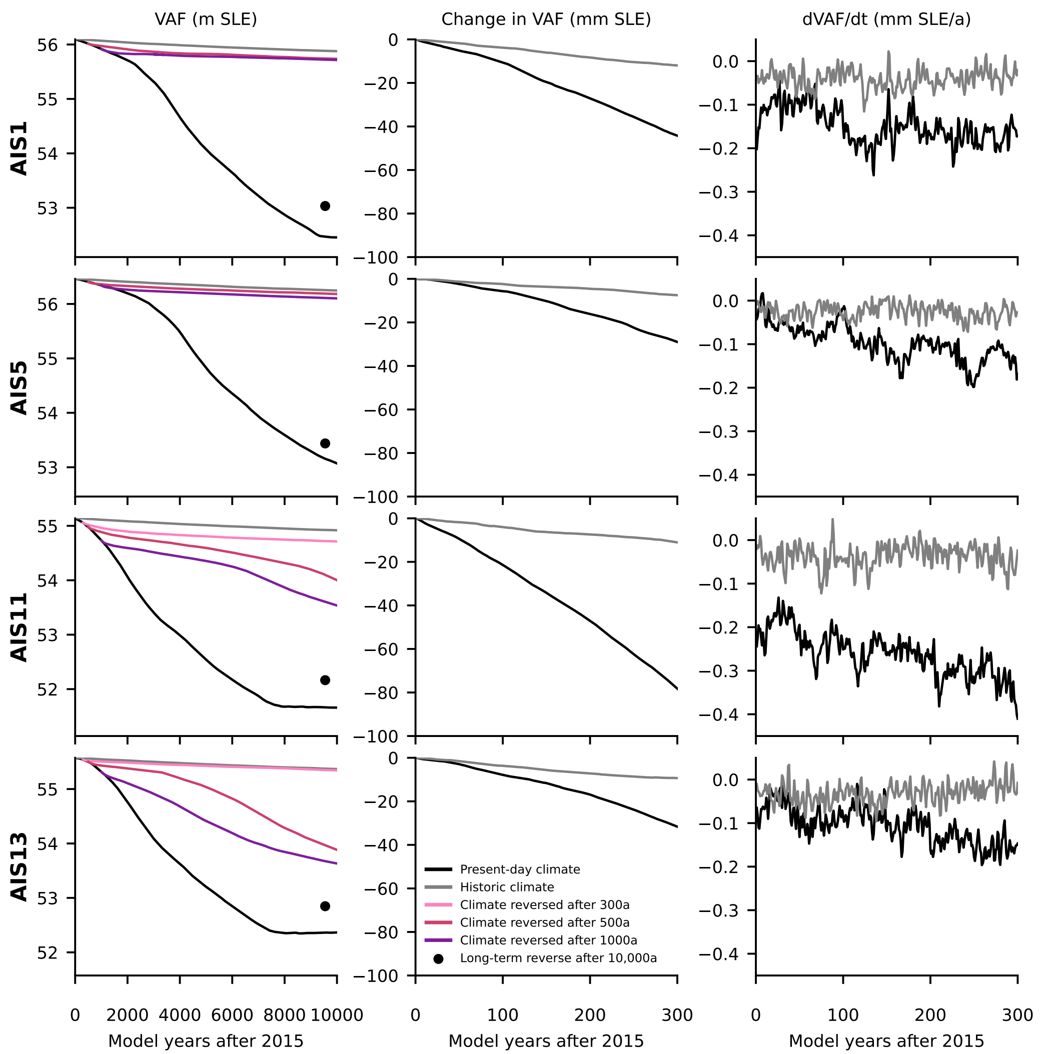

Figure 6. **Evolution of selected ensemble members over 10,000 and 300 years.** Shown is the sea-level relevant ice volume over 10,000 years (left panels), its change over 300 years (middle panels) and the rate of volume change over the 300 years (right panels). We show the evolution for the best ensemble member (AIS1), the best ensemble member for 'mean' PICO parameters (AIS5), and AIS11 and AIS13, two members that show centennial onset of irreversible retreat. Dots in the left panels show the volume above flotation after 20,000 years of reversing to pre-industrial conditions after the 10,000 year continued present-day climate.

4.1 PICO parameter selection

In this paper we have selected PICO parameters such that the sensitivity of sub-shelf melt rates to ocean temperature changes in FRIS and for the ASE ice shelves matches with independent estimates. ~~This approach~~ We applied temperature changes between

-2 and 2 K to obtain the aggregated observed melt rates in each basin of PICO. This range span almost the entire variation of ocean temperatures observed in the Southern Ocean, and large temperature corrections could point to missing assumptions in the melt calculation. However, we are interested here in the ice sheet response, and for the ice sheet it is important to have the correct present-day melt rates as well as the correct increase in melt rates with ocean temperature changes, which is achieved by this method. Note that using temperature corrections makes our approach independent of the input temperatures and thus subjective choices of how to calculate 'far-field' input.

Our approach yields different parameters ~~than~~ to those of previous studies (Reese et al., 2018a, 2020), but also ~~than~~ to those of a recent study ~~(with $\gamma_T^\star = 0.41 \times 10^{-5}$ ms^{-1} and $C = 15.1$ Sv m kg^{-1}; Burgard et al., 2022)~~ (with $\gamma_T^\star = 0.39 \times 10^{-5}$ ms^{-1} and $C = 20.5$ which optimized parameters to match with model simulations of NEMO (Nucleus for European Modelling of the Ocean) under present-day conditions. The earlier studies only used present-day melt rates as targets, not the sensitivity of melt rates which is arguably more important for perturbation experiments or projections. While the NEMO simulations did include variability in the ocean input, one reason for the differences in the parameters could be that the NEMO simulations did not include a similarly strong increase in melting of FRIS, which we use here explicitly for parameter ~~optimization~~optimisation. Furthermore, here we concentrate on those two regions which classify as 'warm and small cavities' and ~~'as~~ as 'cold and large cavities', respectively, while Burgard et al. (2022) ~~optimises~~ optimised parameters for all major ice shelves around Antarctica. Our parameters might hence not be suited for other ice shelves, in particular ice shelves in different regimes, e.g., 'small and cold cavities'. Note that ~~these type~~ the grounded ice streams that drain these types of ice shelves might ~~however~~ not contribute substantially to sea-level in the future. For an idealised cavity, Favier et al. (2019) compared PICO and other melt parameterisations to a coupled model, and found that modelled ice mass loss was comparable.

We conclude that the parameter selection for PICO should be ~~adopted~~ adapted to the aim of the study in which they are applied. Since in our study we find most changes for the ASE sector and the large Filchner-Ronne and Ross ice shelves, we think that our parameter selection procedure with particular focus on these regions is appropriate. The way the parameters are selected, by linearising between present-day ocean temperatures and $+1$ K increased conditions, makes this method also applicable for conducting sea-level projections. ~~As a next step, it would be interesting to test the effect of the uncertainty in the parameters, including uncertainties in the temperature corrections, on the evolution of grounding lines under constant present-day climate conditions, which was besides the aim of this work.~~

4.2 PISM experiments

Here we use a suite of PISM simulations that apply changes from 1850 to 2015 and then keep the present-day climate constant for 10,000 years to address the question of committed retreat under present-day climate conditions. In ~~simulations that show large-scale retreat~~ all simulations we reverse the forcing to 1850 conditions to test for reversibility of the grounding lines.

One caveat of the applied methodology is that we rely on the historic forcing by the general circulation model ~~NorESM~~ NorESM1-M (Bentsen et al., 2013), which was selected by ISMIP6 due to its best performance around Antarctica (Barthel et al., 2020), but might incorrectly represent trends in the atmosphere and ocean in some places ~~incorrectly. In particular, currently no ice mass losses are observed in the Weddell and Ross Seas, however,~~ since coarse-resolution climate models cannot fully resolve the important processes on the continental shelf. Furthermore, PICO coarsely samples water masses north of the ice shelves at the depth of the continental shelf and the CMIP forcing is directly, without any modifications, transferred from offshore into the ice-shelf cavity. This representation of the ocean forcing might explain why we find thinning in ~~these regions~~ the Weddell and Ross Seas through the historic model simulations ~~. In addition to the impact of the forcing from NorESM, the assumption of PICO, that ocean conditions on the continental shelf are directly translated into the ice shelf cavity, could introduce uncertainties~~while observations indicate none of these (Smith et al., 2020), and, in addition, why all runs show grounding lines for Filchner-Ronne and Amery ice shelves that are located seaward of observations. The committed specific patterns of retreat simulated in these regions must be interpreted with caution. However, we can use this modelled retreat to test for reversibility, and we find that large-scale retreat of the grounding lines of Filchner-Ronne Ice Shelf and the western Siple Coast of Ross Ice Shelf is reversible if they are allowed to regrow to their initial geometry. Whether Ross and FRIS could become substantial contributors to sea-level rise in the future, or show tipping behaviour in the ocean (Hellmer et al., 2017; Naughten et al., 2021), is an active field of research. Understanding the committed evolution of both systems at present and under future warming in a coupled configuration would hence be of great interest.

On the other hand, our simulations ~~have a tendency to~~ underestimate present-day mass loss in the ASE sector. This might be explained by ocean forcing that is too weak in comparison to present day, but also other factors, like the horizontal resolution of 8 km in the model simulations, too high snowfall increases, the exclusion of calving and damage from the simulations, or the choice of the friction law. Generally ocean forcing in the Amundsen Sea is a complicated process (Jenkins et al., 2016; Holland et al., 2019) and more work is needed to understand its effect on the stability regime. We keep present-day climate conditions constant, but substantial decadal variability is observed in particular in the Amundsen and Bellingshausen Seas (Jenkins et al., 2018), which is known to influence numerical results (Hoffman et al., 2019).

~~While we find that ice sheet states with more rigid bed do not show committed WAIS collapse under present-day forcing, an increase in ocean temperatures by $+0.3$ already changes that result. Similarly, we find retreat into marine basins upstream of Ross and FRIS to be sensitive to small variations in ocean temperatures. This indicates that only small changes in ocean conditions can have a huge effect on the long-term committed retreat~~Similarly, the biases in the surface mass balance field and their modelled evolution can affect the results. Improved data ~~of~~ on the present-day forcing, and its variability, would be required to further investigate the commitment of WAIS collapse. Our experiments rely on PICO for providing sub-shelf melt rates and RACMO for providing the surface mass balance field. Discrepancy from observations will influence the results and it would hence be interesting in future work to analyse the influence of alternative melt parameterisations, such as a quadratic parameterisation, and alternative surface mass balance fields on the timing and reversibility of grounding line retreat.

Since there is still a small drift in our simulations after 10,000 years, we did not fully identify the stable steady state grounding line position that the 2015 grounding lines in our model are attracted to. All results are hence given with reference to this time frame, but they allow us to analyse the evolution of the system over a rather long period of time. Similar caveats apply for the reversibility simulations, which we maximally ran over 20,000 years to reduce drift in the final states. In addition, our experiments focus on reversibility of large-scale retreat. Smaller events of irreversible retreat might occur that are not distinguishable in the large-scale picture, see Rosier et al. (2021).

We here used an ensemble approach to better understand the influence of ice sheet model parameters on the sensitivity of present-day Antarctic grounding lines. Due to computational constraints, we could not explore the full parameter space. ~~In particular~~Moreover, an important mitigating factor for MISI ~~are gravity-induced~~ is relative sea-level ~~changes~~ change at the grounding line that can be induced through gravity changes (Gomez et al., 2010) as well as glacial isostatic rebound ~~(Gomez et al., 2015)~~(Gomez et al., 2015; Whitehouse et al., 2019). These feedbacks make grounding lines less prone to instability. For ~~consistency~~ creating consistent initial states with the two other models in the companion paper that all include as similar model physics as possible and due to the equilibrium spin-up procedure chosen here, those feedbacks are not accounted for in the PISM experiments. Also for ~~that~~ the first reason, we do not apply calving ~~or adjustments to~~ except for prescribing the ice front at its present location or adjustments of the surface mass balance to surface elevation changes. Note that these modelling choices make it possible to analyse the existence of MISI independently from the above mentioned positive or negative feedback mechanisms. Feedback mechanisms that are included in the simulations are thermomechanical feedbacks between sliding, saturation of the till, englacial strain rates and friction since we let the ice enthalphy and basal till water content evolve in the simulations. ~~Furthermore,~~ Note that calving could influence the stability regime substantially (Haseloff and Sergienko, 2018). Since calving upstream of the current ice front would mostly reduce ice shelf buttressing or not impact it, we would expect that including this process would not affect our finding of large-scale irreversible retreat in the Amundsen Sea under current climate forcing. Results on reversible retreat in our simulations could be affected by more disruptive calving. The way melting is applied at partially floating grid cells is known to influence the results (Seroussi and Morlighem, 2018), and we do thus not apply melting in ~~partially floating cells here~~grounded cells that are partially floating. A study with higher resolution of individual regions could help to understand the effect of potentially prohibiting melting over important regions close to the grounding line.

We start the historic simulations from an equilibrium state in 1850 which does not include the paleoclimate history of the Antarctic Ice Sheet. ~~This~~ That the climate history is not included in modelled temperatures will influence in particular inland ice velocities in slower flowing regions and thus the sensitivity of the grounding line to large-scale retreat. Furthermore, it means that any grounding line retreat that was committed before 1850 cannot be considered in this analysis. However, this approach makes it possible for us to perform a clearly defined analysis of the effect of the recent ice sheet history on its committed grounding line evolution. In their model simulation of the evolution of the Antarctic Ice Sheet since the last interglacial, Golledge et al. (2021) find the WAIS to retreat under current climate conditions. Their simulation includes past-climate influence on englacial temperatures, glacial isostatic adjustment and calving, and is hence complementary to our approach. They do not test for irreversibility. It would be interesting, as a next step, to analyse the ~~effect of the Antarctic Ice Sheet trajectory through the~~ remnant influence of past glacial cycles and ~~deglaciation~~ interglacial climates on the currently committed grounding line retreat (and reversibility of retreat) in more detail.

Finally, we compare our results to previous studies. The timescales over which the WAIS collapses in our simulations are on the order of thousands of years. This timescale is similar to other studies that analyse tipping processes (Garbe et al., 2020; Rosier et al., 202 . The onset of irreversible retreat occurs at different times in the simulations, showing that further work is required to better understand the likelihood of the onset of irreversible retreat in the future. It is known that stronger forcing can increase the rates of mass loss substantially and shorten timescales. For example, following a complete removal of ice shelves, the WAIS was found to collapse within a few centuries (Sun et al., 2020). The volume of committed ice loss we find is similar to previous studies. For example, Golledge et al. (2021) suggest a committed loss of up to 4 m SLE. The maximum mass loss over the next 300 years under constant present-day climate forcing is 0.4 mm/a which is in line with present-day rates (Shepherd et al., 2018) .

4.3 ~~Potential states of~~ Has the (West) Antarctic ~~grounding lines~~Ice Sheet already tipped?

~~**Example for reversibility in 2015.** The simulation ANT7 shows large-scale WAIS retreat and an irreversible collapse of Thwaites Glacier under constant present-day climate conditions (grounding line flux shown in red), see Fig. 5. However, reversing the ocean and atmosphere back to 1850 conditions after 2015 allows the grounding line flux (light blue line) to reverse to the pre-industrial control (grey line) and prevents the collapse. We here show grounding line flux evolution over 500 years as done in Urruty et al. (in review). In Section 4.3.1we discuss a classification of current Antarctic grounding lines~~ To discuss our modelling results in the context of tipping, we here first introduce relevant concepts, see Sect. 4.3.1. Then we discuss the implications of the accompanying paper (Urruty et al., in review) as well as our simulations for the potential qualitative states that Antarctic ice streams or glaciers could be in with respect to MISI~~. We argue that four different grounding line states are possible: MISI exists and neither the critical parameter not the critical system state has been crossed (1, 'no instability') , MISI exists and the critical parameter has been crossed but not the critical system state(2, 'committed instability'), MISI exists and both, the critical system state and the critical parameterhaven been crossed and the grounding line is engaged~~ , see Sect. 4.3.2, and discuss this classification, see Sect. 4.3.3. Note that the terminology used here for nonlinear systems is based on Strogatz (2018).

4.3.1 Theoretical framing

MISI occurs when a positive feedback, where retreat of the grounding line increases the ice flow across the grounding line and this in turn causes further retreat, is at play. For a laterally uniform ice sheet or ice stream, ice flow across the grounding line is a function of the local ice thickness which is linked through the flotation criterion to the bed topography. This means that in such a case and due to the positive feedback, stable steady state grounding-line positions cannot exist on retrograde, in-land sloping beds (assuming constant bed properties and ice rheology; Schoof, 2007, 2012). In the presence of buttressing ice shelves, conditions are more complicated and it is possible that MISI is suppressed (Gudmundsson et al., 2012; Haseloff and Sergienko, . In the absence of buttressing, it was found that also a specific distribution of the basal friction parameter can allow for stable steady state grounding lines on retrograde sloping beds (Brondex et al., 2017). In other words, a retrograde bed slope is a necessary but not sufficient condition for MISI. Numerical modelling is then required to assess the existence and conditions under which MISI occurs. The potential for irreversible grounding-line retreat in regions upstream of present-day grounding lines has been shown in numerical simulations for the whole Antarctic Ice Sheet (Garbe et al., 2020), the West Antarctic Ice Sheet (Feldmann and Levermann, 2015a), the Wilkes subglacial basin in East Antarctica (Mengel and Levermann, 2014), and

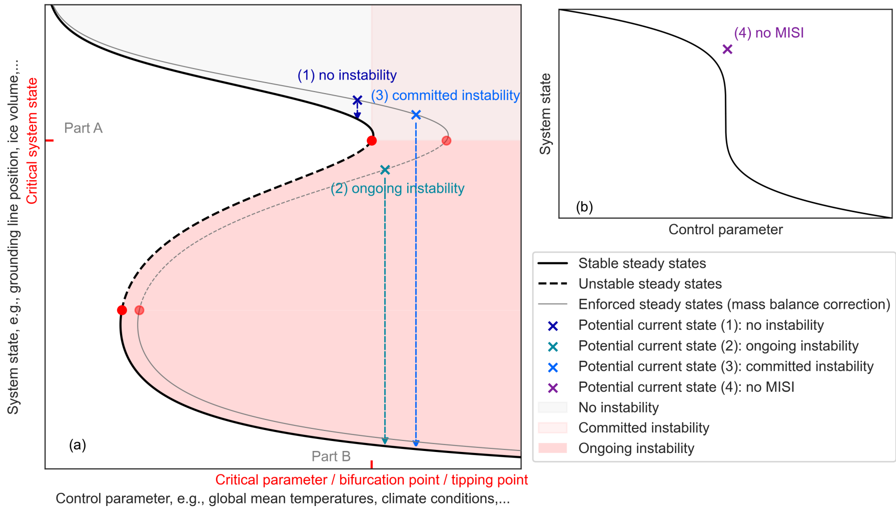

Figure 7. Schematic of potential present-day states of Antarctic grounding lines with respect to MISI. Illustrated is (a) a schematic bifurcation diagram for the Marine Ice Sheet Instability (MISI) and (b) a schematic diagram illustrating a reversible system, both represented by a system state and a control parameter and both showing potential for large-scale transitions. Black curve shows underlying steady system states (solid for stable, dashed for unstable). Bifurcations are indicated by red dots with their critical control parameter (also referred to as bifurcation or tipping point) shown on the x-axis and their corresponding critical system state indicated on the y-axis. If MISI exists (panel a), the current, transient grounding line (indicated by crosses) might be at three qualitatively different locations relative to the steady-state curve and the tipping point. If no MISI exists (panel b), large-scale changes in the system state are reversible. The companion paper, Part A (Urruty et al., in review), assesses whether the grounding line is currently undergoing MISI, by enforcing a steady state using a mass balance correction (grey curve). In this paper, Part B, we analyse the long-term evolution of the grounding lines (indicated by arrows relative to the black curves) and their reversibility, i.e., whether large-scale retreat might be committed under constant climate forcing and if so, if this retreat is reversible.

using high resolution modelling with an in-depth tipping analysis for Pine Island Glacier in the ASE sector (Rosier et al., 2021) . The existence of irreversible retreat for other grounding lines requires further investigation.

MISI gives rise to hysteresis behaviour (Schoof, 2007) which can be visualised in a bifurcation diagram showing the system state, e.g., current location of the grounding line, with respect to the relevant control parameter, e.g., climate forcing in the atmosphere and ocean, see Fig. 7. Hysteresis means that over a range of control parameter values, several possible steady system states exist and thus the (evolution of the) current system state depends on its history. Those steady system states, or grounding line positions, can be stable or unstable, depending on whether a small-amplitude perturbation to the system is dampened (stable) or amplified (unstable) so that the system evolves back to its original steady state or away from it. At the threshold value of the control parameter, a stable and an unstable branch merge. If the control parameter is moved beyond that (bifurcation/tipping) point, the system will engage in an irreversible ~~retreat (3, 'ongoing instability'), no MISI exists and all perturbations are reversible (4, 'no MISI').~~ transition towards the only existing stable system state. Moving the control parameter across a tipping point is how tipping in marine ice sheets is generally thought to occur (this is called bifurcation-induced tipping, alternative ways of tipping are discussed e.g., in Vanselow et al., 2022). Such a transition is called 'irreversible', since reverting back to the original system state requires the control parameter to be reduced substantially below the tipping point value until a second tipping point is crossed and the system irreversibly changes back to the first state. See Rosier et al. (2021) for a more detailed discussion.

~~Our reversibility experiments show that MISI exists for Thwaites Glacier, which is in line with previous findings for the ASE (Feldmann and Levermann, 2015a) and excludes case (4). The experiments further show that grounding lines in Filchner-Ronne and Ross ice shelves are reversible, indicating them to be in state (4). This is in line with a modelling study finding a stable grounding line positionon a retrograde sloping bed (Gudmundsson et al., 2012). This~~ We hypothesise that glaciers, ice streams as well as marine basins of the Antarctic Ice Sheet with overdeepened beds show 'slow-onset' tipping (Ritchie et al., 2021). This would mean that it is possible to have a temporary overshoot of the control parameter, i.e., climate conditions, above the tipping point without forcing the grounding lines to enter irreversible retreat, i.e., WAIS collapse. Such a mechanism has been described for other systems as affording 'borrowed time' in which it is possible to revert to previous conditions before the undesirable system state locks in (Hughes et al., 2013). It is plausible since under very slowly increasing control parameters in quasi-steady experiments the ice sheet's system state was found to evolve above the equilibrium curve, see Garbe et al. (2020) and Rosier et al. (2021). As the ice stream or glacier takes a long time to adjust to changes in the climate conditions, the grounding line movement 'lags behind'. However, the mechanical, positive feedback related to MISI can only kick in once the grounding line retreats on a retrograde sloping bed.

An Antarctic ice stream whose grounding line has been forced to retreat by a loss in ice-shelf buttressing and for which MISI is possible based on flowline theory (e.g., which has a retrograde sloping bed upstream) could hence be in one of the four qualitative positions in terms of MISI (see Fig. 7):

1. **No instability:** the ice stream has one (or several) tipping point related to MISI, but the tipping points have not been crossed. Letting the grounding line evolve with the control parameter (climate) kept constant, it would reach a stable steady state not too far inland from its current position, i.e., remain on the upper stable branch (following the dark blue arrow in panel (a)). This state is not tipped.

2. **Ongoing instability:** the grounding line is ~~buttressed (Gudmundsson, 2013) and grounding lines in Filchner-Ronne and Ross ice shelves were reported to show even stronger buttressing (Reese et al., 2018c). Also, theoretical work by Pegler (2018) and Haseloff and Sergienko (2018) did show that strong buttressing can suppress MISI . In our experiments we allow the ice shelves to regrow to their current extent.Haseloff and Sergienko (2018) showed that in the presence of buttressing, also the calving law influences the stability regime of grounding lines , and the implication of the calving law on the reversibility of~~ currently undergoing irreversible retreat after crossing a tipping point related to MISI. When evolving this system forward under constant climate conditions, the grounding line retreats further until it reaches a new stable steady state branch (following the turquoise arrow in panel (a)). This retreat is irreversible, i.e., reducing the

climate conditions back to the pre-tipping value is not sufficient to stop the retreat. Such a state is considered to be tipped.

3. **Committed tipping:** the ice stream has a tipping point related to MISI, and the control parameter has crossed the corresponding tipping point, but the grounding line has not yet engaged in irreversible retreat. Under constant climate conditions, the grounding line will eventually enter irreversible retreat (following the light blue arrow in panel (a)), but this retreat could still be prevented by reducing the control parameter below its critical value. Such a state is considered to be ‘not tipped yet’.

4. **No MISI:** the ice stream has no tipping point related to MISI. The system might show large-scale changes for small changes in the control parameter, but these are reversible when the control parameter is reversed (panel (b)).

4.3.2 Potential states of present-day Antarctic grounding lines with respect to MISI

The numerical analysis of our companion paper (Urruty et al., in review) shows that MISI is likely not occurring at any of the Antarctic grounding lines at present. In that paper, a balance approach is used by which the surface mass balance is modified so that the current Antarctic grounding lines are in steady state (schematically indicated by the grey curve in Fig. 7a). Then, their stability is tested in a numerical stability analysis. If an unstable steady state was found, then the grounding line would likely be undergoing MISI in its current position, indicating state (2). However, a stable steady state was found for all grounding lines with respect to the modified surface mass balance, which indicates that the grounding lines are likely not undergoing MISI in their current positions or that no MISI exists. This can be interpreted as case (1), (3) or (4) being true. The present paper investigates the question of whether the current Antarctic grounding lines ~~should be explored further~~are more likely to represent case (1), (3) or (4).

We first discuss the ASE sector. Our reversibility experiments show that MISI exists for Thwaites Glacier, and, similarly, for Pine Island Glacier, which is in line with previous findings (Favier et al., 2014; Feldmann and Levermann, 2015a; Rosier et al., 2021) and excludes case (4). That the ‘overshoot’ state (~~2~~3) indeed exists for Antarctic grounding lines becomes clear from our experiments: ~~we test one state that shows~~ our Antarctic configurations show a long-term ~~committed~~ irreversible collapse in Thwaites Glacier, i.e., that it could be in state (2) or (3) ~~, and~~ and not in (1), and when we reverse the forcing after the historic simulation until 2015 and another 300 years of constant present-day climate back to the 1850 climate conditions~~. This run shows reversibility(see Fig. 6) . This state is hence indeed~~, all runs show reversibility, excluding case (2) in line with Urruty et al. (in review). The current grounding line of Thwaites could hence indeed be a case (~~2~~3) state and the ~~committed~~ collapse can still be reversed in present-day. ~~This is further underlined by running the perturbation experiments from Urruty et al. (in review) in which we find no indication of MISI-driven retreatin the 2015 geometry, see Fig. ??.~~ We have similar findings for PIG, although overall retreat is less pronounced.

We now discuss the Filchner-Ronne and Ross ice shelves. Urruty et al. (in review) hints at state (2) being unlikely, in line with our reversibility experiments showing no continued retreat in these regions when reversing the climate to pre-industrial conditions after 300 years. Our long-term, constant-climate experiments expose a large part of the marine basins upstream of both ice shelves that is likely unrealistic as discussed in Sect. 4.2. However, it allows to test for reversibility in case of such large-scale retreat. In our experiments, grounding lines in Filchner-Ronne and Ross ice shelves are in most areas reversible, indicating them to be in state (4) and not in (1), (2) or (3). However, hysteresis could be possible but the climate forcing changes so much in the experiments that it ‘jumps’ over the loop, i.e., we cannot exclude the other states on the basis of our experiments. Reversibility, or case (4), would be consistent with numerical modelling and theoretical findings of stable grounding line position on retrograde sloping beds in the presence of buttressing, as discussed in Sect. 4.3.1, since grounding lines in Filchner-Ronne and Ross ice shelves were reported to show strong buttressing (Reese et al., 2018c).

Other grounding lines show no large-scale retreat in our experiments. They are thus neither in state (2) nor (3) according to our simulations. ~~If~~ Distinguishing whether they are in state (1) or (4) ~~cannot be concluded from our runs~~ is not possible in our experiments and more work would be needed to understand their potential for irreversible retreat. ~~Overall, our results underline that observations of grounding line retreat cannot be interpreted as indications of irreversible retreat or collapse. Instead, dedicated numerical experiments are required to understand the underlying stability regime.~~

~~We want to note that our experiments in this paper do not directly test for the onset of MISI, but if the final retreat over large marine basins is reversible.~~

4.3.3 Discussion of classification of potential states

~~Furthermore, since there is still a small drift in our simulations after 10,000 years, we did not fully identify the underlying stable steady state grounding line position. Further retreat is possible, and also those simulations that show no collapse could theoretically still show retreat and collapse after year 12,000. All results are hence given with reference to this time frame, but they allow us to analyse the tendency of the evolution of the system over a rather long period of time. Similar caveats apply for the re-advance simulations, which we ran over 20,000 years to reduce drift in the final states. In addition, our experiments focus on reversibility of large-scale retreat. Smaller tipping points might occur and be not distinguishable in the large-scale picture, see Rosier et al. (2021).~~

Our classification of Antarctic grounding lines (Sect. 4.3.1 and 4.3.2) is based on the assumption that steady state positions exist. Since ice dynamics ~~is~~ are also influenced by thermodynamics, ~~also~~ oscillatory or limit cycle behaviour is also possible. In this case the system would not settle on one stable steady state if run forward under constant conditions, but on a closed, oscillatory attractor (e.g., Feldmann and Levermann, 2017). However, a previous study that ~~includes~~ included thermodynamics (Garbe et al., 2020) generally showed hysteresis behaviour for Antarctica on a broad scale, so we think that making this assumption is appropriate here. Similarly, other previous studies assessing the long-term (thousands to millions of years) hysteresis behaviour of the Antarctic Ice Sheet also show stable steady state behaviour, with ~~cycle behaviour only induced by (cyclic) insolation forcing~~ cyclic behaviour only simulated in response to a cyclic external forcing (e.g., insolation changes on orbital timescales) rather than an internal process (e.g., Pollard and DeConto, 2005; Langebroek et al., 2009). This is also underlined by our control run experiments which show convergence of their ice volume towards steady states rather than ~~large scale~~ large-scale cyclic behaviour. ~~Other feedbacks and processes than MISI might~~ Feedbacks and processes other than MISI will influence the stability regime of grounding lines, e.g., bedrock uplift and the melt-elevation feedback can lead to cyclic behaviour (Zeitz et al., 2021)~~. We hereexclude those feedbacks and only focus on MISI~~, which are not considered here.

~~The timescales over which the WAIS collapses in our runs, are thousands of years. This timescale is similar to other studies that analyse tipping processes (Garbe et al., 2020; Rosier et al., 2021; Feldmann and Levermann, 2015a; Mengel and Levermann, 2014) . However, stronger forcing can increase the rates of mass loss substantially and shorten time scales. For example, following a complete removal of ice shelves ,~~ Haseloff and Sergienko (2018) showed that, in the presence of buttressing, the ~~WAIS was found to collapse within a few centuries (Sun et al., 2020). Also, the volume of committed ice loss we find is similar to previous studies. For example, Golledge et al. (2021) suggest a committed loss of up to 4 m SLE~~calving law influences the stability regime of grounding lines. Therefore, noting that ice shelves in our experiments were permitted to regrow to their previous extent without calving, the influence of the calving law on the states of Antarctic grounding lines should be explored further. As discussed in Sect. 4.2, we note however, that more aggressive calving would not affect our finding of large scale, committed, and irreversible retreat in the Amundsean Sea under current climate. However, our numerical experiments exclude alternative feedbacks and only focus on MISI, see Sect. 4.2. Since mitigating processes are not considered in our experiments, we cannot conclude that MISI will definitively occur under current climate conditions, even though our experiments indicate that Amundsen Sea glaciers are in a 'not tipped yet' state with respect to MISI. Rather, our experiments indicate that under current climate the onset of irreversible retreat in the Amundsen Sea in the future cannot be excluded.

5 Conclusions

~~In this manuscript we aim to understand the current state~~ Using an ensemble of numerical simulations with PISM, we analyse the evolution of Antarctic grounding lines ~~by analysing their underlying steady states and the reversibility of large-scale transitions if they occur.~~ under present-day climate conditions. Currently the ice sheet is not in steady state, and it will therefore continue to evolve for some time until a steady state is reached. Since recent modelling and observations suggest that a change in sub-shelf melt rates is ~~thought to be~~ a major trigger for grounding line retreat in Antarctica, we present a new parameter optimisation approach for the ~~melt rate~~ sub-shelf melt parameterisation PICO. This approach ensures that the sensitivity of melt rates to ocean temperature changes is in accordance with observations or high-resolution ocean simulations. This makes the parameters also suitable for sea-level projections. ~~Using an ensemble of numerical simulations with PISM, we analyse the evolution of Antarctic grounding lines under present-day climate conditions. We find that for some possible representations in our ensemble,~~

Using these new parameters, we find that as the Antarctic Ice Sheet approaches a new steady state for current climate conditions~~can force a retreat of Thwaites Glacier in the ASE sector which eventually results in an irreversible collapse. Note that this is not contradictory to the finding in the companion paper that grounding lines in Antarctica are currently not engaged in MISI (Urruty et al., in review): grounding lines can be in an 'overshoot' state or state of 'committed instability' since grounding lines adjust to external forcing over long timescales of centuries to millennia. In this state they are not engaged in a MISI yet and their retreat is still reversible, but they might evolve towards an instability if climate conditions are kept constant. Our~~

~~experimentsshow that for some ensemble members, Thwaites Glacier is in such a state. Furthermore, we find that large-scale retreat of the grounding lines of Filchner-Ronne and Ross ice shelves is reversible if they are allowed to regrow to their initial geometry. Overall, retreat of grounding lines in the ASE sector, in Filchner-Ronne and Ross ice shelves is found to be very sensitive to subtle changes in model parameters or ocean conditions while all other grounding lines remain at a steady state close to their current position in all present-day model configurations. An improved assessment of the predictive capabilities of large-scale ice sheet models over long timescalescould help to reduce the range of admissible parameters and thereby uncertainties in the grounding line evolution. Further observations and coupled simulations of ice sheet and ocean models could help to provide a deeper analysis and to quantify the probability of large-scale retreat or committed instability today and under future warming. Importantly, committed instability means that a collapse is not irreversible yet; rather,~~, the grounding lines migrate inland in West Antarctica, but remain close to their current positions in East Antarctica. In all our runs, the grounding line enters phases of accelerated retreat in the Amundsean Sea. By conducting reversibility experiments, we have been able to demonstrate that these retreat phases are irreversible. We find that the timescale at which irreversible retreat starts is dependent on the model parameters of the initial configuration. None of our runs shows the onset of irreversible retreat within the first 300 years, but three of fifteen runs show an onset between 300 and 500 years. In all runs, the collapse evolves over millennial timescales, leading eventually to 2.7 to 3.5 m of sea-level rise. We find that the rate of the ~~grounding lines are in a state of 'overshoot' – and if, and how fast, the collapse occurs in the future depends on how climate conditions evolve~~Antarctic Ice Sheet sea level contribution is limited to 0.9 $\mathrm{mm/a}$, including periods of accelerated, irreversible retreat.

Our modelling work hence suggests that the Antarctic Ice Sheet will eventually enter periods of self-enhancing and irreversible retreat, as it evolves over time from its current unsteady state towards a steady state. As this tipping behaviour is found in our model simulations under constant climatic forcing corresponding to current day conditions, and does not required any future changes in climate, we refer to this as "committed tipping". However, while (in this sense) committed, the tipping is not inevitable: future changes in external climate forcing as well as mitigating processes such as glacial isostatic rebound could accelerate, delay, or even suppress the crossing of tipping points altogether. Further narrowing down the conditions for the onset of tipping, and changes in external conditions required to suppress it, will require further work.

Appendix A: PICO

A1 Melt sensitivity for Filchner-Ronne Ice Shelf

We estimate the sensitivity of average melt rates to ocean warming for Filchner-Ronne Ice Shelf using an ocean model simulation described in Naughten et al. (2021). In the simulation a coupled setup of the ocean model MITgcm (Marshall et al., 1997; Losch, 2008) and the ice-sheet model Úa (Gudmundsson et al., 2012) for the Weddell Sea is forced by an abrupt quadrupling of CO2 in the atmosphere. Antarctic surface and oceanic boundary conditions are provided by UKESM (Met Office Hadley Centre (2019), 5.4.2022). We use the 'abrupt-4xCO2' experiment from the standard CMIP6 protocol for UKESM, and repeat the last 10 years 5 times to extend the simulation to be 200 years long. In this simulation, the FRIS cavity undergoes a two-step response, first salinity decreases which also reduces melting, then warm Circumpolar Deep Water enters the cavity and

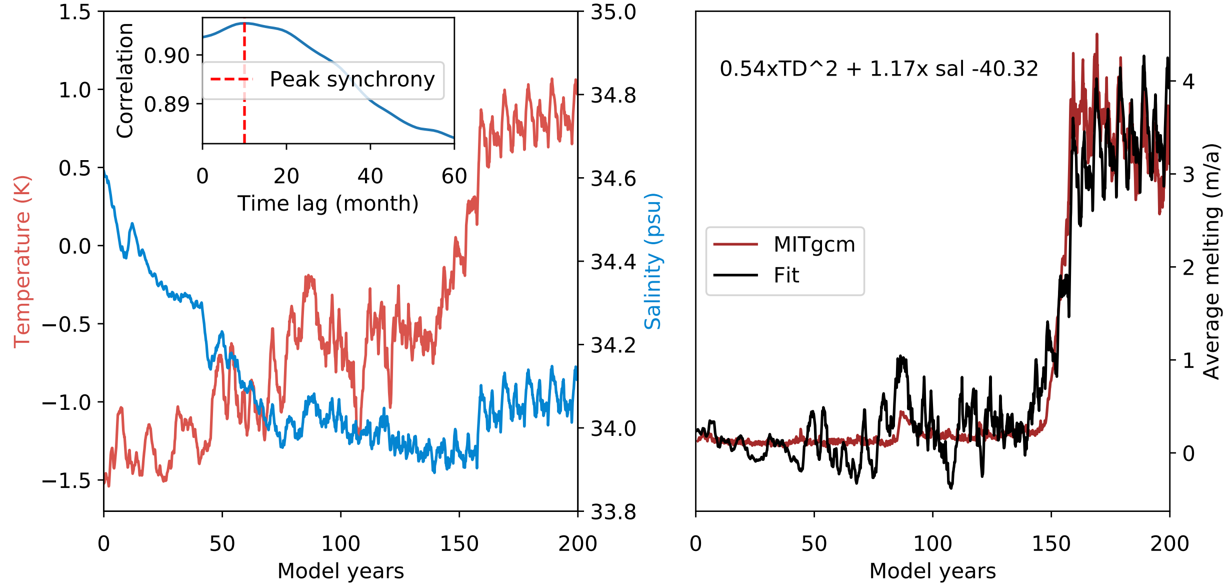

Figure A1. Filchner-Ronne Ice Shelf melt relationship estimate. Left panel: evolution of average ocean temperature and salinity at the depth of the continental shelf in front of the ice shelf in the ocean simulations of the Weddell Sea in Naughten et al. (2021) for the abrupt quadrupling of CO2. Inset shows correlation values for estimating the time-lag between shelf-wide averaged melt and ocean temperatures on the continental shelf. Right panel: modelled and predicted melt rates using the fitted function with parameters described in the figure.

drives an order of magnitude increase in melting, see Fig. A1. As this simulation spans a wide range of basal melt and ocean temperature forcing, we use it to derive the melt sensitivity of FRIS.

To this aim, we relate temperatures at the depth of the continental shelf in MITgcm with melting at the ice ocean interface. Using the average temperature over continental shelf in front of FRIS is a rough assumption which neglects complex processes that influence the in- and outflow of water masses in that cavity. However, it reflects best the assumptions and forcing used in PICO. First, we estimate the time the water masses on the continental shelf need to circulate into the cavity to drive melting using a cross-correlation. We find that a time-lag of 10 months yields the highest correlation between the temperature signal and the melt signal, see inset in Fig. A1. Then, we fit a function to the modelled data of thermal driving, salinity and melt rates using least-squares. We expect the melt rates to also depend on salinity because the salinity gradient between the continental shelf and the cavity controls the strength of circulation, which in turn affects the melt rate. We assume that the (time-shifted) melt depends quadratically on thermal driving (as discussed in Section 2.2) and linearly on salinity. Note that we assume a linear dependency on salinity as we are not aware of a more specific functional relationship. The R-squared value of the fit is 0.937 and the P-values for the coefficients are smaller than 0.0005, so we consider this sufficiently good. The resulting, predicted melt rates show a similar pattern of increase as the modelled melt rates, see right panel of Fig. A1. Differences arise since this fit cannot capture the complicated physical processes in the Weddell Sea. This also shows when we use the fitted relationship to predict melt in the alternative scenario from Naughten et al. (2021) that is based on a 1 percent increase in

Table A1. Baseline thermal driving for FRIS and the ASE region. Values are relative to the surface freezing point.

	$TD_{mean}(^{\circ}\mathrm{C})$	$TD_{min}(^{\circ}\mathrm{C})$	$TD_{max}(^{\circ}\mathrm{C})$	Citation
FRIS 4xCO2 (first 30 years)	0.53	0.35	0.84	Naughten et al. (2021)
FRIS historic	0.26	0.13	0.47	Naughten et al. (2021)
FRIS observations	0.14			Schmidtko et al. (2014)
PIG observations	1.85	1.42	2.22	Dutrieux et al. (2014)
DIS observations	1.38	1.04	1.84	Jenkins et al. (2018)
ASE observations	2.34			Schmidtko et al. (2014)

FRIS = Filchner Ronne Ice Shelf, PIG = Pine Island Glacier Ice Shelf, DIS = Dotson Ice Shelf, ASE = Amundsen Sea Embayment sector.

CO2, see Fig. S7. While we can capture about the order of magnitude of melt rate increase, the fitted model amplifies the trend in melting too much and produces too large variability. Also in the end of the abrupt quadrupling of CO2 (after year 160), the fitted function predicts increasing melt rates, because temperature and salinity slightly increase, while modeled melt rates slightly decrease. However, the fit is able to reproduce the large-scale pattern of the melt increase.

A2 Selection of baseline temperatures

We here describe the selection of baseline thermal driving (temperatures relative to the surface freezing point) to linearise the sensitivity between the selected thermal driving value and a warming of 1 K. The linearised sensitivity hence applies to current ocean temperatures and captures also a warming of around 1 K. While a sensitivity that is linearised around present-day (plus minus half a degree or going one degree below present-day) would be better suited for the historic simulations carried out in this paper, the increase from present-day levels was chosen since the numerical stability analysis of present-day grounding lines in the companion paper (Urruty et al., in review) is tested by increasing ocean temperatures above present-day levels. It also makes the sensitivity estimates suitable for projections of the Antarctic sea-level contribution over the coming century. Note that if ocean temperatures change by more than one degree, for example in simulations over longer time scales, the quadratic relationship implies that PICO, which has a linear relationship, underestimates melt rate changes.

Table A1 shows a compilation of thermal driving values from modelling and observations. For FRIS, we list the min, mean and max of the first 30 years of the 4xCO2 simulation with low melt rates and conditions comparable to present-day, the historic simulation from 1979 to 2014 and the value from Schmidtko et al. (2014) as given in Reese et al. (2018a). For the Amundsen Sea, we use the min and max from the observations for PIG and DIS together with the value from Schmidtko et al. (2014) as given in Reese et al. (2018a).

We use the minimum and maximum of all values for an upper and lower range of sensitivities. For the best estimate of FRIS, we use the mean of the FRIS 4xCO2 simulation which is $0.53^{\circ}\mathrm{C}$. This makes the baseline thermal driving consistent with the fitted sensitivity curve. It is warmer than the average from the data in Schmidtko et al. (2014), so yields a slightly larger sensitivity, which is however still smaller than sensitivities estimated from other studies, see Sect. 2.2. For the best estimate

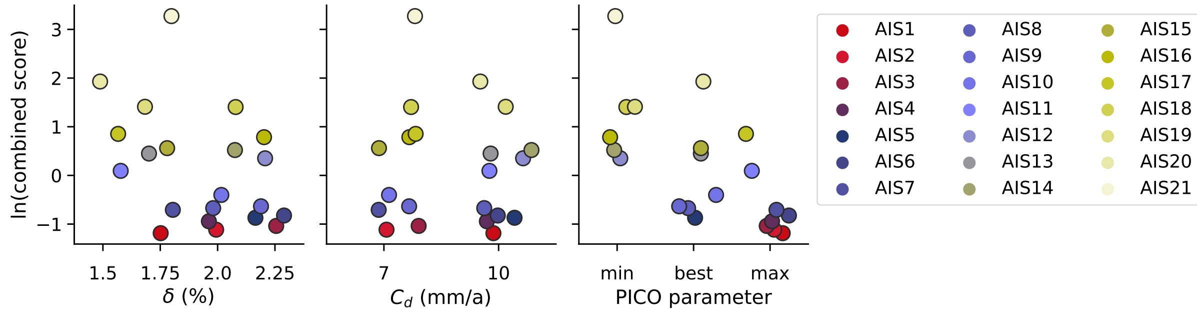

Figure B1. Scoring of ensemble of initial configurations in 2015. Scores are based on observed ice thickness, velocities, mass loss, grounding line positions, and a special focus is given to the Amundsen, Ross and Weddell seas. Initial ensemble members were obtained from equilibrium simulations of a full parameter ensemble with ~~the best five~~ all runs ~~for the entire AIS, the Amundsen, Weddell and Ross seas~~ that showed grounding lines broadly in agreement with present-day continued after 5000 to full 25,000 years (total of ~~16~~ 21 runs). ~~From these 9 runs were selected and for~~ For each a historic simulation was run from 1850 to 2015. The 2015 state is then scored with present-day observations. Shown is the natural logarithm of the scores. The lower the values the better the agreement with present-day.

in the ASE region, we use an average over available observational temperatures for DIS, PIG and the whole region, which is $1.65°$C. This value is lower than the estimate in Schmidtko et al. (2014) and hence the sensitivity is slightly lower. It is however in line with sensitivity estimates from other studies, see Sect. 2.2, and the higher value is included as the maximum sensitivity estimate.

Appendix B: PISM simulations

We show the scoring for the initial configurations in 2015 (Fig. B1), and the long-term evolution of the control simulations (Fig. B2).

Code availability. PISM code is publicly available at https://github.com/pism/pism (last access: 5.4.2022). We plan to submit PISM simulations and python plotting scripts to the open access repository zenodo if the manuscript gets published.

Author contributions. In cooperation with all members of the TiPACCs work package 2, RR designed the study, ran the simulations with PISM and wrote the manuscript. JG supported the plotting. KN provided and processed the FRIS ocean model simulation data used for fitting the quadratic sensitivity curve. All authors contributed to the writing and discussion of ideas.

Competing interests. All authors declare that they have no competing interests.

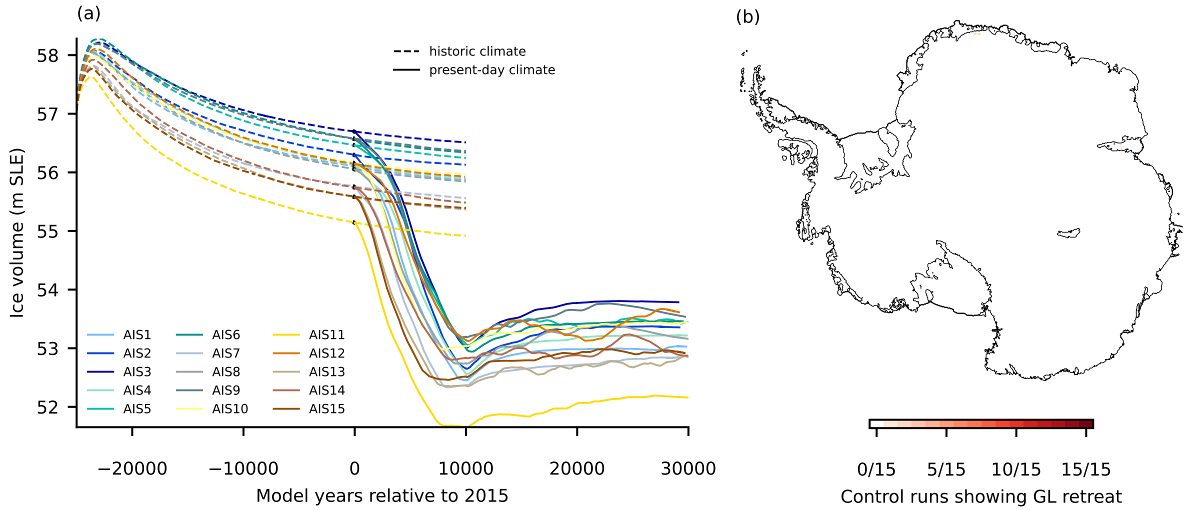

Figure B2. **~~Control runs.~~** **Sea level evolution and control runs.** Panel (a) shows the evolution of Antarctic Ice Sheet volume (in meters sea-level equivalent, m SLE) during the control runs and the simulations with constant present-day climate conditions and the reverse to historic conditions for all ensemble members used in the manuscript. Black dots show historic control from 1850 to 2015. Dashed lines show control runs, solid lines show the simulations with constant present-day forcing. Panel (b) shows the regions that unground in the control runs between 1850 and year 12,~~000.~~015 (hardly any). The ~~grey~~ black line is the BedMachine grounding line.

Acknowledgements. This work is part of the TiPACCs project, which receives funding from the European Union's Horizon 2020 research and innovation programme under grant agreement no. 820575. Development of PISM is supported by NASA grant NNX17AG65G and NSF grants PLR-1603799 and PLR-1644277. The authors gratefully acknowledge the European Regional Development Fund (ERDF), the German Federal Ministry of Education and Research and the Land Brandenburg for supporting this project by providing resources on the high performance computer system at the Potsdam Institute for Climate Impact Research.

We would like to thank Christian Schoof for providing helpful input on stability analysis and Chris Bull and Adrian Jenkins for helpful discussions on the PICO parameter selection.

References

Adusumilli, S., Fricker, H. A., Medley, B., Padman, L., and Siegfried, M. R.: Interannual variations in meltwater input to the Southern Ocean from Antarctic ice shelves, Nature Geoscience, 13, 616–620, https://doi.org/10.1038/s41561-020-0616-z, 2020.

Albrecht, T., Winkelmann, R., and Levermann, A.: Glacial-cycle simulations of the Antarctic Ice Sheet with the Parallel Ice Sheet Model (PISM)–Part 2: Parameter ensemble analysis, The Cryosphere, 14, 633–656, 2020.

Arthern, R. J. and Williams, C. R.: The sensitivity of West Antarctica to the submarine melting feedback, Geophysical Research Letters, 44, 2352–2359, 2017.

Aschwanden, A., Bueler, E., Khroulev, C., and Blatter, H.: An enthalpy formulation for glaciers and ice sheets, Journal of Glaciology, 58, 441–457, 2012.

Barthel, A., Agosta, C., Little, C. M., Hattermann, T., Jourdain, N. C., Goelzer, H., Nowicki, S., Seroussi, H., Straneo, F., and Bracegirdle, T. J.: CMIP5 model selection for ISMIP6 ice sheet model forcing: Greenland and Antarctica, The Cryosphere, 14, 855–879, 2020.

Bentsen, M., Bethke, I., Debernard, J. B., Iversen, T., Kirkevåg, A., Seland, Ø., Drange, H., Roelandt, C., Seierstad, I. A., Hoose, C., et al.: The Norwegian earth system model, NorESM1-M—Part 1: Description and basic evaluation of the physical climate, Geosci. Model Dev, 6, 687–720, 2013.

Blankenship, D. D., Bentley, C. R., Rooney, S., and Alley, R. B.: Till beneath Ice Stream B: 1. Properties derived from seismic travel times, Journal of Geophysical Research: Solid Earth, 92, 8903–8911, 1987.

Brondex, J., Gagliardini, O., Gillet-Chaulet, F., and Durand, G.: Sensitivity of grounding line dynamics to the choice of the friction law, Journal of Glaciology, 63, 854–866, 2017.

Brondex, J., Gillet-Chaulet, F., and Gagliardini, O.: Sensitivity of centennial mass loss projections of the Amundsen basin to the friction law, The Cryosphere, 13, 177–195, 2019.

Bueler, E. and Brown, J.: Shallow shelf approximation as a "sliding law" in a thermomechanically coupled ice sheet model, Journal of Geophysical Research: Solid Earth, 114, 1–21, https://doi.org/10.1029/2008JF001179, 2009.

Bueler, E. and van Pelt, W.: Mass-conserving subglacial hydrology in the Parallel Ice Sheet Model version 0.6, Geoscientific Model Development, 8, 1613–1635, 2015.

Burgard, C., Jourdain, N. C., Reese, R., Jenkins, A., and Mathiot, P.: An assessment of basal melt parameterisations for Antarctic ice shelves, The Cryosphere Discussions, pp. 1–56, 2022.

Comeau, D., Asay-Davis, X. S., Begeman, C. B., Hoffman, M. J., Lin, W., Petersen, M. R., Price, S. F., Roberts, A. F., Van Roekel, L. P., Veneziani, M., et al.: The DOE E3SM v1. 2 Cryosphere Configuration: Description and Simulated Antarctic Ice-Shelf Basal Melting, Journal of Advances in Modeling Earth Systems, 14, e2021MS002 468, 2022.

Dutrieux, P., Rydt, J. D., Jenkins, A., Holland, P. R., Ha, H. K., Lee, S. H., Steig, E. J., Ding, Q., Abrahamsen, E. P., and Schroder, M.: Strong Sensitivity of Pine Island Ice-Shelf Melting to Climatic Variability, Science, 343, 174–178, https://doi.org/10.1126/science.1244341, 2014.

Engelhardt, H. and Kamb, B.: Basal hydraulic system of a West Antarctic ice stream: constraints from borehole observations, Journal of Glaciology, 43, 207–230, 1997.

Favier, L., Durand, G., Cornford, S., Gudmundsson, G., Gagliardini, O., Gillet-Chaulet, F., Zwinger, T., Payne, A., and Le Brocq, A.: Retreat of Pine Island Glacier controlled by marine ice-sheet instability, Nature Climate Change, 4, 117–121, https://doi.org/doi:10.1038/nclimate2094, 2014.

Favier, L., Jourdain, N. C., Jenkins, A., Merino, N., Durand, G., Gagliardini, O., Gillet-Chaulet, F., and Mathiot, P.: Assessment of sub-shelf melting parameterisations using the ocean–ice-sheet coupled model NEMO (v3. 6)–Elmer/Ice (v8. 3), Geoscientific Model Development, 12, 2255–2283, 2019.

Feldmann, J. and Levermann, A.: Collapse of the West Antarctic Ice Sheet after local destabilization of the Amundsen Basin, Proceedings of the national academy of sciences, 112, 14 191–14 196, ~~2015.~~ 2015a.

Feldmann, J. and Levermann, A.: Interaction of marine ice-sheet instabilities in two drainage basins: simple scaling of geometry and transition time, The Cryosphere, 9, 631–645, 2015b.

Feldmann, J. and Levermann, A.: From cyclic ice streaming to Heinrich-like events: the grow-and-surge instability in the Parallel Ice Sheet Model, The Cryosphere, 11, 1913–1932, 2017.

Feldmann, J., Albrecht, T., Khroulev, C., Pattyn, F., and Levermann, A.: Resolution-dependent performance of grounding line motion in a shallow model compared with a full-Stokes model according to the MISMIP3d intercomparison, Journal of Glaciology, 60, 353–360, 2014.

Garbe, J., Albrecht, T., Levermann, A., Donges, J. F., and Winkelmann, R.: The hysteresis of the Antarctic ice sheet, Nature, 585, 538–544, 2020.

Golledge, N. R., Clark, P. U., He, F., Dutton, A., Turney, C., Fogwill, C., Naish, T., Levy, R. H., McKay, R. M., Lowry, D. P., et al.: Retreat of the Antarctic Ice Sheet during the Last Interglaciation and implications for future change, Geophysical Research Letters, 48, e2021GL094 513, 2021.

Gomez, N., Mitrovica, J. X., Huybers, P., and Clark, P. U.: Sea level as a stabilizing factor for marine-ice-sheet grounding lines, Nature Geoscience, 3, 850–853, 2010.

Gomez, N., Pollard, D., and Holland, D.: Sea-level feedback lowers projections of future Antarctic Ice-Sheet mass loss, Nature communications, 6, 1–8, 2015.

~~Gudmundsson, G.: Ice-shelf buttressing and the stability of marine ice sheets, The Cryosphere, 7, 647–655, 2013.~~

Gudmundsson, G. H., Krug, J., Durand, G., Favier, L., and Gagliardini, O.: The stability of grounding lines on retrograde slopes, The Cryosphere, 6, 1497–1505, https://doi.org/10.5194/tc-6-1497-2012, 2012.

Gudmundsson, G. H., Paolo, F. S., Adusumilli, S., and Fricker, H. A.: Instantaneous Antarctic ice sheet mass loss driven by thinning ice shelves, Geophysical Research Letters, 46, 13 903–13 909, 2019.

Haseloff, M. and Sergienko, O. V.: The effect of buttressing on grounding line dynamics, Journal of Glaciology, 64, 417–431, 2018.

Hellmer, H. H., Kauker, F., Timmermann, R., Determann, J., and Rae, J.: Twenty-first-century warming of a large Antarctic ice-shelf cavity by a redirected coastal current, Nature, 485, 225–228, 2012.

Hellmer, H. H., Kauker, F., Timmermann, R., and Hattermann, T.: The fate of the southern Weddell Sea continental shelf in a warming climate, Journal of Climate, 30, 4337–4350, 2017.

Hoffman, M. J., Asay-Davis, X., Price, S. F., Fyke, J., and Perego, M.: Effect of subshelf melt variability on sea level rise contribution from Thwaites Glacier, Antarctica, Journal of Geophysical Research: Earth Surface, 124, 2798–2822, 2019.

Holland, P. R., Jenkins, A., and Holland, D. M.: The Response of Ice Shelf Basal Melting to Variations in Ocean Temperature, Journal of Climate, 21, 2558–2572, https://doi.org/10.1175/2007jcli1909.1, 2008.

Holland, P. R., Bracegirdle, T. J., Dutrieux, P., Jenkins, A., and Steig, E. J.: West Antarctic ice loss influenced by internal climate variability and anthropogenic forcing, Nature Geoscience, 12, 718–724, 2019.

Hughes, T. P., Linares, C., Dakos, V., Van De Leemput, I. A., and Van Nes, E. H.: Living dangerously on borrowed time during slow, unrecognized regime shifts, Trends in ecology & evolution, 28, 149–155, 2013.

Jenkins, A.: A one-dimensional model of ice shelf-ocean interaction, Journal of Geophysical Research: Oceans, 96, 20 671–20 677, https://doi.org/10.1029/91JC01842, 1991.

Jenkins, A., Dutrieux, P., Jacobs, S., Steig, E. J., Gudmundsson, G. H., Smith, J., and Heywood, K. J.: Decadal ocean forcing and Antarctic ice sheet response: Lessons from the Amundsen Sea, Oceanography, 29, 106–117, 2016.

Jenkins, A., Shoosmith, D., Dutrieux, P., Jacobs, S., Kim, T. W., Lee, S. H., Ha, H. K., and Stammerjohn, S.: West Antarctic Ice Sheet retreat in the Amundsen Sea driven by decadal oceanic variability, Nature Geoscience, 11, 733–738, https://doi.org/10.1038/s41561-018-0207-4, 2018.

Joughin, I., Smith, B. E., and Medley, B.: Marine ice sheet collapse potentially under way for the Thwaites Glacier Basin, West Antarctica, Science, 344, 735–738, 2014.

Jourdain, N. C., Asay-Davis, X., Hattermann, T., Straneo, F., Seroussi, H., Little, C. M., and Nowicki, S.: A protocol for calculating basal melt rates in the ISMIP6 Antarctic ice sheet projections, The Cryosphere, 14, 3111–3134, https://doi.org/10.5194/tc-14-3111-2020, 2020.

Langebroek, P. M., Paul, A., and Schulz, M.: Antarctic ice-sheet response to atmospheric CO 2 and insolation in the Middle Miocene, Climate of the Past, 5, 633–646, 2009.

Losch, M.: Modeling ice shelf cavities in azcoordinate ocean general circulation model, Journal of Geophysical Research, 113, https://doi.org/10.1029/2007jc004368, 2008.

Marshall, J., Hill, C., Perelman, L., and Adcroft, A.: Hydrostatic, quasi-hydrostatic, and nonhydrostatic ocean modeling, Journal of Geophysical Research: Oceans, 102, 5733–5752, https://doi.org/10.1029/96jc02776, 1997.

~~Martin, M. A., Winkelmann, R., Haseloff, M., Albrecht, T., Bueler, E., Khroulev, C., and Levermann, A.: The Potsdam Parallel Ice Sheet Model (PISM-PIK) – Part 2: Dynamic equilibrium simulation of the Antarctic ice sheet, The Cryosphere, 5, 727–740, , 2011.~~

Mengel, M. and Levermann, A.: Ice plug prevents irreversible discharge from East Antarctica, Nature Climate Change, 4, 451–455, 2014.

Mercer, J. H.: West Antarctic ice sheet and CO 2 greenhouse effect: a threat of disaster, Nature, 271, 321–325, 1978.

Met Office Hadley Centre (2019): WCRP CMIP6: Met Office Hadley Centre (MOHC) UKESM1-0-LL model output for the "abrupt-4xCO2" experiment, Centre for Environmental Data Analysis, 5.4.2022.

Milillo, P., Rignot, E., Rizzoli, P., Scheuchl, B., Mouginot, J., Bueso-Bello, J., Prats-Iraola, P., and Dini, L.: Rapid glacier retreat rates observed in West Antarctica, Nature Geoscience, pp. 1–6, 2022.

Morlighem, M., Rignot, E., Binder, T., Blankenship, D., Drews, R., Eagles, G., Eisen, O., Ferraccioli, F., Forsberg, R., Fretwell, P., et al.: Deep glacial troughs and stabilizing ridges unveiled beneath the margins of the Antarctic ice sheet, Nature Geoscience, 13, 132–137, 2020.

Mouginot, J., Rignot, E., and Scheuchl, B.: Sustained increase in ice discharge from the Amundsen Sea Embayment, West Antarctica, from 1973 to 2013, Geophysical Research Letters, 41, 1576–1584, 2014.

Mouginot, J., Rignot, E., and Scheuchl, B.: Continent-wide, interferometric SAR phase, mapping of Antarctic ice velocity, Geophysical Research Letters, 46, 9710–9718, 2019.

Naughten, K. A., Rydt, J. D., Rosier, S. H. R., Jenkins, A., Holland, P. R., and Ridley, J. K.: Two-timescale response of a large Antarctic ice shelf to climate change, Nature Communications, 12, https://doi.org/10.1038/s41467-021-22259-0, 2021.

Olbers, D. and Hellmer, H.: A box model of circulation and melting in ice shelf caverns, Ocean Dynamics, 60, 141–153, 2010.

~~Paolo, F. S., Fricker, H. A., and Padman, L.: Volume loss from Antarctic ice shelves is accelerating, Science, 348, 327–331, 2015.~~

Payne, A. J., Holland, P. R., Shepherd, A. P., Rutt, I. C., Jenkins, A., and Joughin, I.: Numerical modeling of ocean-ice interactions under Pine Island Bay's ice shelf, Journal of Geophysical Research, 112, https://doi.org/10.1029/2006jc003733, 2007.

Pegler, S. S.: Suppression of marine ice sheet instability, Journal of Fluid Mechanics, 857, 648–680, 2018.

Pollard, D. and DeConto, R. M.: Hysteresis in Cenozoic Antarctic ice-sheet variations, Global and Planetary Change, 45, 9–21, 2005.

Reese, R., Albrecht, T., Mengel, M., Asay-Davis, X., and Winkelmann, R.: Antarctic sub-shelf melt rates via PICO, The Cryosphere, 12, 1969–1985, https://doi.org/10.5194/tc-12-1969-2018, 2018a.

Reese, R., Albrecht, T., Mengel, M., Asay-Davis, X., and Winkelmann, R.: Antarctic sub-shelf melt rates via PICO, The Cryosphere, 12, 1969–1985, 2018b.

Reese, R., Winkelmann, R., and Gudmundsson, G. H.: Grounding-line flux formula applied as a flux condition in numerical simulations fails for buttressed Antarctic ice streams, The Cryosphere, 12, 3229–3242, 2018c.

Reese, R., Levermann, A., Albrecht, T., Seroussi, H., and Winkelmann, R.: The role of history and strength of the oceanic forcing in sea level projections from Antarctica with the Parallel Ice Sheet Model, The Cryosphere, 14, 3097–3110, https://doi.org/10.5194/tc-14-3097-2020, 2020.

Rignot, E., Mouginot, J., Morlighem, M., Seroussi, H., and Scheuchl, B.: Widespread, rapid grounding line retreat of Pine Island, Thwaites, Smith, and Kohler glaciers, West Antarctica, from 1992 to 2011, Geophysical Research Letters, 41, 3502–3509, 2014.

Rignot, E., Mouginot, J., Scheuchl, B., Van Den Broeke, M., Van Wessem, M. J., and Morlighem, M.: Four decades of Antarctic Ice Sheet mass balance from 1979–2017, Proceedings of the National Academy of Sciences, 116, 1095–1103, 2019.

~~Ritchie, P., Karabacak, Ö., and Sieber, J.: Inverse-square law between time and amplitude for crossing tipping thresholds, Proceedings of the Royal Society A, 475, 20180 504, 2019.~~

Ritchie, P. D., Clarke, J. J., Cox, P. M., and Huntingford, C.: Overshooting tipping point thresholds in a changing climate, Nature, 592, 517–523, 2021.

Rosier, S. H., Reese, R., Donges, J. F., De Rydt, J., Gudmundsson, G. H., and Winkelmann, R.: The tipping points and early warning indicators for Pine Island Glacier, West Antarctica, The Cryosphere, 15, 1501–1516, 2021.

~~Scheffer, M., Bascompte, J., Brock, W. A., Brovkin, V., Carpenter, S. R., Dakos, V., Held, H., Van Nes, E. H., Rietkerk, M., and Sugihara, G.: Early-warning signals for critical transitions, Nature, 461, 53–59, 2009.~~

Schmidtko, S., Heywood, K. J., Thompson, A. F., and Aoki, S.: Multidecadal warming of Antarctic waters, Science, 346, 1227–1231, https://doi.org/10.1126/science.1256117, 2014.

Schoof, C.: Ice sheet grounding line dynamics: Steady states, stability, and hysteresis, Journal of Geophysical Research: Earth Surface, 112, 2007.

Schoof, C.: Marine ice sheet stability, Journal of Fluid Mechanics, 698, 62, 2012.

Seroussi, H. and Morlighem, M.: Representation of basal melting at the grounding line in ice flow models, The Cryosphere, 12, 3085–3096, 2018.

Seroussi, H., Nakayama, Y., Larour, E., Menemenlis, D., Morlighem, M., Rignot, E., and Khazendar, A.: Continued retreat of Thwaites Glacier, West Antarctica, controlled by bed topography and ocean circulation, Geophysical Research Letters, 44, 6191–6199, https://doi.org/10.1002/2017gl072910, 2017.

Seroussi, H., Nowicki, S., Payne, A. J., Goelzer, H., Lipscomb, W. H., Abe-Ouchi, A., Agosta, C., Albrecht, T., Asay-Davis, X., Barthel, A., Calov, R., Cullather, R., Dumas, C., Galton-Fenzi, B. K., Gladstone, R., Golledge, N. R., Gregory, J. M., Greve, R., Hattermann, T., Hoffman, M. J., Humbert, A., Huybrechts, P., Jourdain, N. C., Kleiner, T., Larour, E., Leguy, G. R., Lowry, D. P., Little, C. M., Morlighem, M., Pattyn, F., Pelle, T., Price, S. F., Quiquet, A., Reese, R., Schlegel, N.-J., Shepherd, A., Simon, E., Smith, R. S., Straneo, F., Sun, S., Trusel, L. D., Breedam, J. V., van de Wal, R. S. W., Winkelmann, R., Zhao, C., Zhang, T., and Zwinger, T.: ISMIP6 Antarctica: a multi-model ensemble of the Antarctic ice sheet evolution over the 21st century, The Cryosphere, 14, 3033–3070, https://doi.org/10.5194/tc-14-3033-2020, 2020.

Shepherd, A., Ivins, E., Rignot, E., Smith, B., Van Den Broeke, M., Velicogna, I., Whitehouse, P., Briggs, K., Joughin, I., Krinner, G., et al.: Mass balance of the Antarctic Ice Sheet from 1992 to 2017, Nature, 558, 219–222, 2018.

Smith, A., Anker, P., Nicholls, K., Makinson, K., Murray, T., Rios-Costas, S., Brisbourne, A., Hodgson, D., Schlegel, R., and Anandakrishnan, S.: Ice stream subglacial access for ice-sheet history and fast ice flow: the BEAMISH Project on Rutford Ice Stream, West Antarctica and initial results on basal conditions, Annals of Glaciology, 62, 203–211, 2021.

Smith, B., Fricker, H. A., Gardner, A. S., Medley, B., Nilsson, J., Paolo, F. S., Holschuh, N., Adusumilli, S., Brunt, K., Csatho, B., et al.: Pervasive ice sheet mass loss reflects competing ocean and atmosphere processes, Science, 368, 1239–1242, 2020.

Strogatz, S. H.: Nonlinear dynamics and chaos: with applications to physics, biology, chemistry, and engineering, CRC press, 2018.

Sun, S., Pattyn, F., Simon, E. G., Albrecht, T., Cornford, S., Calov, R., Dumas, C., Gillet-Chaulet, F., Goelzer, H., Golledge, N. R., et al.: Antarctic ice sheet response to sudden and sustained ice-shelf collapse (ABUMIP), Journal of Glaciology, 66, 891–904, 2020.

Taylor, K. E., Stouffer, R. J., and Meehl, G. A.: An overview of CMIP5 and the experiment design, Bulletin of the American meteorological Society, 93, 485–498, 2012.

Urruty, B., Hill, E., Reese, R., Garbe, J., Gagliardini, O., Durand, G., Gillet-Chaulet, F., Gudmundsson, G. H., Winkelmann, R., Chekki, M., Chandler, D., and Langebroek, P. M.: The stability of present-day Antarctic grounding lines — Part A: No indication of marine ice sheet instability in the current geometry, The Cryosphere, in review.

van Wessem, J. M., van de Berg, W. J., Noël, B. P. Y., van Meijgaard, E., Amory, C., Birnbaum, G., Jakobs, C. L., Krüger, K., Lenaerts, J. T. M., Lhermitte, S., Ligtenberg, S. R. M., Medley, B., Reijmer, C. H., van Tricht, K., Trusel, L. D., van Ulft, L. H., Wouters, B., Wuite, J., and van den Broeke, M. R.: Modelling the climate and surface mass balance of polar ice sheets using RACMO2 – Part 2: Antarctica (1979–2016), Cryosphere, 12, 1479–1498, https://doi.org/10.5194/tc-12-1479-2018, 2018.

Vanselow, A., Halekotte, L., and Feudel, U.: Evolutionary rescue can prevent rate-induced tipping, Theoretical Ecology, 15, 29–50, 2022.

Weertman, J.: Stability of the junction of an ice sheet and an ice shelf, Journal of Glaciology, 13, 3–11, 1974.

Whitehouse, P. L., Gomez, N., King, M. A., and Wiens, D. A.: Solid Earth change and the evolution of the Antarctic Ice Sheet, Nature communications, 10, 1–14, 2019.

Winkelmann, R., Martin, M. A., Haseloff, M., Albrecht, T., Bueler, E., Khroulev, C., and Levermann, A.: The Potsdam parallel ice sheet model (PISM-PIK)–Part 1: Model description, The Cryosphere, 5, 715–726, 2011.

Zeitz, M., Haacker, J. M., Donges, J. F., Albrecht, T., and Winkelmann, R.: Dynamic regimes of the Greenland Ice Sheet emerging from interacting melt-elevation and glacial isostatic adjustment feedbacks, Earth System Dynamics Discussions, pp. 1–25, 2021.